Mitochondria-Targeted Doxorubicin: A New Therapeutic Strategy against Doxorubicin-Resistant Osteosarcoma

Mitochondria-targeted doxorubicin: a new therapeutic strategy against doxorubicin-resistant osteosarcoma

Ilaria Buondonno[1], Elena Gazzano[1], Sae Rin Jean[2,3], Valentina Audrito[4,5], Joanna Kopecka[1], Marilù Fanelli[6], Iris C. Salaroglio[1], Costanzo Costamagna[1], Ilaria Roato[7], Eleonora Mungo[1], Claudia M. Hattinger[6], Silvia Deaglio[4,5], Shana O. Kelley[2,3], Massimo Serra[6], Chiara Riganti[1]

[1] Department of Oncology, University of Torino, via Santena 5/bis, 10126, Torino, Italy

[2] Department of Pharmaceutical Sciences, Leslie Dan Faculty of Pharmacy, University of Toronto, 144 College Street, M5S 3M2, Toronto, ON, Canada

[3] Department of Chemistry, Faculty of Arts and Science, University of Toronto, 80 St. George Street, M5S 3H6, Toronto, ON, Canada

[4] Human Genetics Foundation (HuGeF), via Nizza 52, 10126, Torino, Italy

[5] Department of Medical Sciences, University of Torino, corso Dogliotti 14, 10126, Torino, Italy

[6] Orthopaedic Rizzoli Institute, Laboratory of Experimental Oncology, Pharmacogenomics and Pharmacogenetics Research Unit, via Giulio Cesare Pupilli 1, 40136, Bologna, Italy

[7] Center for Research and Experimental Medicine (Ce.R.M.S.), San Giovanni Battista Hospital, via Santena 5/bis, 10126, Torino, Italy

Running title: Targeting mitochondria in drug-resistant osteosarcoma

Keywords: doxorubicin, osteosarcoma, P-glycoprotein, mitochondria, drug resistance

Abbreviations list: Dox, doxorubicin; ABC, ATP binding cassette; Pgp, P-glycoprotein; MRP1, multidrug resistance related protein 1; mtDox, mitochondria-targeted doxorubicin; FITC, fluorescein isothiocyanate; GFP, green fluorescence protein; LDH, lactate dehydrogenase; HMGB1,

high mobility group box 1; MFI, mean fluorescence intensity; DC, dendritic cell; AST; aspartate aminotransferase; ALT, alanine aminotransferase; AP, alkaline phosphatase; CPK, creatine phosphokinase; COX-I, subunit I of complex IV; SDH-A, succinate dehydrogenase-A; PGC-1α, peroxisome proliferator-activated receptor gamma coactivator-1α; TCA, tricarboxylic acid cycle; ASM, acid soluble metabolites; AICAR, 5-aminoimidazole-4-carboxamide ribonucleotide; OCR, oxygen consumption rate; FCCP; carbonyl cyanide 4-(trifluoromethoxy) phenylhydrazone; ROS, reactive oxygen species; DCFDA-AM, 5-(and-6)-chloromethyl-2',7'-dichlorodihydro-fluorescein diacetate-acetoxymethyl ester; ANOVA, analysis of variance; MTD, maximum tolerated dose; SOD, superoxide dismutase; ER, endoplasmic reticulum; MAM, ER-membrane-associated to mitochondria; CS, collateral sensitivity.

Notes

Corresponding author: Dr. Chiara Riganti, Department of Oncology, University of Torino, via Santena 5/bis, 10126, Torino, Italy; phone: +390116705857; fax: +390116705845; email: chiara.riganti@unito.it

Financial information

This work was supported with funds from Italian Association for Cancer Research (IG15232 to C. Riganti) and Italian Ministry of University and Research (FIRB 2012, grant RBFR12SOQ1 to C. Riganti); Canadian Institutes for Health Research Operating Grant (to S.O. Kelley); 5‰ contributions to Rizzoli Institute (to M. Serra). I. Buondonno and I.C. Salaroglio are recipients of PhD scholarships from the Italian Institute for Social Security (INPS). E. Gazzano is recipient of a post-doctoral fellowship from the Italian Ministry of University and Research. V. Audrito is recipient of the #15047 fellowship from the Italian Association for Cancer Research/Italian

Foundation for Cancer Research (FIRC). J. Kopecka is recipient of a fellowship from “Fondazione Umberto Veronesi”.

The funding institutions had no role in the study design, in the data collection and analysis, or in writing the manuscript.

Disclosure of Potential Conflicts of Interests

The authors declare that they have no conflicts of interests.

Total words count: 5246 words

Total number of figures and tables: 6

Abstract

Doxorubicin is one of the leading drugs for osteosarcoma standard chemotherapy. 40-45% of high grade osteosarcoma patients are unresponsive, or only partially responsive, to doxorubicin, due to the overexpression of the drug efflux transporter ABCB1/P-glycoprotein (Pgp). The aim of this work is to improve doxorubicin-based regimens in resistant osteosarcomas. We used a chemically modified mitochondria-targeted doxorubicin (mtDox) against Pgp-overexpressing osteosarcomas with increased resistance to doxorubicin. Unlike doxorubicin, mtDox accumulated at significant levels intracellularly, exerted cytotoxic activity, induced necrotic and immunogenic cell death in doxorubicin-resistant/Pgp-overexpressing cells, fully reproducing the activities exerted by anthracyclines in drug-sensitive tumors. mtDox reduced tumor growth and cell proliferation, increased apoptosis, primed tumor cells for the recognition by the host immune system and was less cardiotoxic than doxorubicin in pre-clinical models of drug-resistant osteosarcoma. The increase in doxorubicin resistance was paralleled by a progressive upregulation of mitochondrial metabolism. By widely modulating the expression of mitochondria-related genes, mtDox decreased mitochondrial biogenesis, the import of proteins and metabolites within mitochondria, mitochondrial metabolism and the synthesis of ATP. These events were paralleled by increased reactive oxygen species production, mitochondrial depolarization and mitochondria-dependent apoptosis in resistant osteosarcoma cells, where doxorubicin was completely ineffective.

We propose mtDox as a new effective agent with a safer toxicity profile compared to doxorubicin that may be effective for the treatment of doxorubicin-resistant/Pgp-positive osteosarcoma patients, who strongly need alternative and innovative treatment strategies.

Introduction

Osteosarcoma is the most frequent bone tumor observed clinically. The standard treatment for conventional osteosarcoma (tumors, which are not metastatic at clinical onset, with high grade malignancy, located at the extremities in patients younger than 40 years) is based on pre- and post-operative chemotherapy, including doxorubicin (Dox), cisplatin and methotrexate. This treatment is successful in about 55%-60% of patients. Despite numerous attempts to find new therapeutic approaches for osteosarcoma, the patients' prognosis has not improved in the last decades (1, 2 and references therein). The main drawbacks of Dox are the onset of drug resistance that makes chemotherapy progressively ineffective (2) and the onset of cardiotoxicity (3).

Dox is a substrate of ATP binding cassette (ABC) transporters, such as ABCB1/P-glycoprotein (Pgp) and ABCC1/multidrug resistance related protein 1 (MRP1), which efflux the drug outside the tumor cell and limit its cytotoxicity (4). The presence of Pgp in osteosarcoma patients is a negative prognostic factor and is predictive of poor response to treatment (5-8). Both natural (9, 10) and synthetic (11, 12) inhibitors of Pgp have been tested to reverse Dox resistance in osteosarcoma cell lines *in vitro*. The specific silencing of Pgp (13) or the inhibition of pathways involved in drug resistance – such as the hypoxia inducible factor-1α- (14) or polo-like kinase 1-dependent signaling (15) – appear to be promising strategies, but the translation of these approaches to clinical settings is still under investigation.

Recently, targeting mitochondria of osteosarcoma cells has been proposed as an effective therapeutic strategy (16). On the other hand, since the heart has an aerobic mitochondria-based metabolism, mitochondria-targeting drugs - while effective on tumor cells - may produce serious cardiotoxicity.

We recently developed chemically-modified Dox derivatives with mitochondrial tropism that are effective against drug-resistant tumor cells overexpressing Pgp (17, 18). One of these mitochondria-targeted Dox compounds (mtDox; 18), did not elicit cardiotoxicity in animals, showing a safer toxicity profile compared to Dox (19).

In this work, we used mtDox against Pgp-overexpressing osteosarcomas *in vitro* and *in vivo* and found that it was significantly more effective and less cardiotoxic than Dox, and that it overcame drug resistance by exploiting the metabolic signature typical of drug-resistant osteosarcoma cells. Our data indicate mtDox as a very promising new chemotherapeutic drug for a possible clinical application in Dox-unresponsive patients.

Materials and methods

Chemicals. Fetal bovine serum and culture medium were from Invitrogen Life Technologies (Carlsbad, CA). Plasticware for cell cultures was from Falcon (Becton Dickinson, Franklin Lakes, NJ). The protein content in cell monolayers, mitochondrial and nuclear extracts was assessed with the BCA kit from Sigma Chemical Co. (St. Louis, MO). Electrophoresis reagents were obtained from Bio-Rad Laboratories (Hercules, CA). Dox was purchased by Sigma Chemical Co. mtDox (Supplementary Figure S1) was synthesized as described in (18). Unless otherwise specified, all the other reagents were purchased from Sigma Chemical Co.

Cell lines. Murine osteosarcoma K7M2 cells, human Dox-sensitive osteosarcoma U-2OS and Saos-2 cells, rat neonatal H9c2 cardiomyocytes were purchased from ATCC (Manassas, VA) in 2012. The corresponding variants with increasing resistance to Dox (U-2OS/DX30, U-2OS/DX100, U-2OS/DX580, Saos-2/DX30, Saos-2/DX100, Saos-2/DX580), selected by culturing parental cells in a medium with 30, 100, 580 ng/mL Dox, were generated as reported in (20). All cell lines were authenticated by microsatellite analysis, using the PowerPlex kit (Promega Corporation, Madison, WI; last authentication: September 2015). Mesenchymal stem cells, derived by discarded lipoaspirates of healthy subject, were cultured in osteogenic condition to obtain primary non-transformed osteoblasts (21, 22). 14 days after culture, Bone Alkaline Phosphatase (BAP staining kit, Sigma Chemicals Co.) was performed, as authentication test for osteoblasts (last authentication: April 2016). Cells were maintained in medium supplemented with 10% v/v fetal bovine serum, 1%

v/v penicillin-streptomycin, 1% v/v L-glutamine. Drug-resistant variants were continuously cultured in presence of Dox.

Cell viability and proliferation. Cell viability was measured by the neutral red staining method, as previously reported (23). The absorbance of untreated cells was considered as 100% viability; the results were expressed as a percentage of viable cells versus untreated cells. To determine IC_{50}, reported in Supplementary Table S1, 1 x 10^5 cells were incubated for 72 h with increasing concentrations of Dox or mtDox (from 1 nmol/L to 1 mmol/L). IC_{50} was considered the concentration of the drug that reduced cell viability to 50%. Cell cycle analysis was measured by flow cytometry, after propidium iodide staining (24).

ABCB1/Pgp and ABCC1/MRP1 expression. For flow cytometry assays, cells were harvested, washed once in PBS, twice with 10 mmol/L Hepes in Hank's balanced salt solution, fixed with 4% paraformaldehyde in PBS for 5 min. After a wash in Hepes, cells were permeabilized in 0.1% w/v saponin and incubated with an anti-ABCB1/Pgp (clone MRK16; Kamiya, Seattle, WA) or anti-ABCC1/MRP1 (clone MRPm5; Abcam, Cambridge, UK) antibodies. After washing with saponin, cells were incubated with a secondary anti-mouse fluorescein isothiocyanate (FITC)-conjugated antibody (Sigma Chemical Co.), washed twice with saponin and once with Hepes. In the negative control, primary antibody was replaced by 0.1% saponin. Samples were analyzed by flow cytometry (FACSCalibur, Becton Dickinson). For Western blot analysis, 20 μg of proteins from cell lysates were probed with anti-Pgp (clone 17F9; BD Biosciences, San Josè, CA) or anti-β-tubulin (clone D-10; Santa Cruz Biotechnology Inc., Santa Cruz, CA) antibodies.

Confocal microscope analysis. 5 x 10^5 cells were grown on sterile glass coverslips and transfected with the green fluorescence protein (GFP)-E1α pyruvate dehydrogenase expression vector (Cell Light BacMan 2.0, Invitrogen Life Technologies) to label mitochondria. After 24 h cells were incubated with 5 μmol/L Dox or mtDox for 6 h. Samples were rinsed with PBS, fixed with 4% w/v paraformaldehyde for 15 min, washed three times with PBS and once with water, mounted with 4 μL of Gel Mount Aqueous Mounting. Slides were analysed using an Olympus FV300 laser

scanning confocal microscope (Olympus Biosystems, Hamburg, Germany; ocular lens: 10X; objective: 60X). For each experimental condition, a minimum of 5 microscopic fields were examined.

Isolation of mitochondria and nuclea. Mitochondria were isolated as reported in (25). A 50 µL aliquot was sonicated and used for the measurement of protein content or Western blotting; the remaining part was stored at -80°C until use. To confirm the presence of mitochondrial proteins in the extracts, 10 µg of each sonicated sample were subjected to SDS-PAGE and probed with an anti-porin antibody (clone 20B12AF2; Abcam). To exclude any mitochondrial contamination in the cytosolic extracts, the absence of porin in the latter was analyzed by Western blotting. Nuclear proteins were extracted using the Nuclear Extract Kit (Active Motif, Rixensart, Belgium). To exclude any cytosolic contamination in the nuclear extracts, the absence of actin (#A2066; Sigma Chemical Co.) in the latter was analyzed by Western blotting.

Doxorubicin accumulation. Cellular, nuclear or mitochondrial extracts were re-suspended in 0.5 mL ethanol/0.3 N HCl. The amount of Dox was measured fluorimetrically (17). Fluorescence was converted into nmol/mg cellular, nuclear or mitochondrial proteins, using a previously set calibration curve.

Necrotic and immunogenic death assays. The activity of lactate dehydrogenase (LDH) released in the extracellular medium, taken as index of necrotic cell death, was measured spectrophotometrically(26). The results were expressed as the percentage of extracellular LDH activity versus total (intracellular + extracellular) LDH activity. To evaluate the immunogenic cell death induced by Dox, the extracellular release of ATP was measured by a chemiluminescence-based assay, the extracellular release of high mobility group box 1 (HMGB1) protein was measured by Western blotting. Following a procedure commonly used in the immunoblotting of extracellular proteins (27), we stained the blot with Red Ponceau and reported a band at the same level of the HMGB1 band, as the control of equal protein loading. Surface translocation of calreticulin, detected

by flow cytometry, was measured (27). The mean fluorescence intensity (MFI) was calculated using Cell Quest software (Becton Dickinson).

Tumor cell phagocytosis. Murine dendritic cells (DC) were obtained as reported by Obeid *et alia* (28). Tumor cell phagocytosis was performed by flow cytometry (28). In each set of experiments, a phagocytosis assay was performed by co-incubating DCs and tumor cells at 4°C, instead of 37°C, and the percentage of phagocytized cells at 4°C was subtracted from values observed at 37°C. The phagocytosis rate was expressed as a phagocytic index, calculated as previously reported (28).

***In vivo* tumor growth, hematochemical parameters and immunohistochemical analysis.** 1 x 10^6 K7M2 cells, stably transfected with the pGL4.51[luc2/CMV/Neo] Vector (Promega Corporation), mixed with 100 µL Matrigel, were injected s.c. in 6 week-old female BALB/c mice (weight: 20 g $\pm$ 1.3; Charles River Laboratories Italia, Calco); 1 x 10^7 U-2OS cells, mixed with 100 µL Matrigel, were injected s.c. in 6 week-old female NOD SCID BALB/c mice (weight: 19.6 g $\pm$ 1.6; Charles River Laboratories Italia). Animals were housed (5 per cage) under 12 h light/dark cycles, with food and drinking provided *ad libitum*. Tumor growth was measured daily by caliper and calculated according to the equation $(LxW^2)/2$, where L = tumor length; W = tumor width. When the tumor reached a volume of 50 mm^3 (day 7 after injection), the mice were randomized into 3 groups: 1) Control group, treated with 0.1 mL saline solution i.v. on days 7, 14, 21, 28; 2) Dox group, treated with Dox i.v. on days 7, 14, 21, 28; 3) mtDox group, treated with mitochondria-targeting Dox i.v. on days 7, 14, 21, 28. *In vivo* bioluminescence imaging was performed on days 7, 21, 35 with a Xenogen IVIS Spectrum (PerkinElmer, Waltham, MA). Tumor volumes were monitored daily by caliper and animals were euthanized by injecting zolazepam (0.2 mL/kg) and xylazine (16 mg/kg) i.m. at day 35. The inhibition rate was calculated as a percentage (i.e. the tumor weight of the control group minus that of the tumor weight of the test group) divided by the tumor weight of the control group. The hematochemical parameters LDH, aspartate aminotransferase (AST), alanine aminotransferase (ALT), alkaline phosphatase (AP), creatinine, creatine phosphokinase (CPK) were measured on 0.5 mL of blood collected immediately after mice sacrifice, using the respective kits

from Beckman Coulter Inc. (Miami, FL). For immunohistochemical analysis, tumors were resected and fixed in 4% v/v paraformaldehyde. The paraffin sections were stained with hematoxylin/eosin, or immunostained for Ki67 (AB9260; Millipore, Billerica, MA), cleaved caspase 3 (#9661, Asp175; Cell Signaling Technology Inc., Danvers, MA), calreticulin (#PA3900; Affinity Bioreagents, Golden, CO), CD11c (clone HL3; BD Biosciences), followed by a peroxidase-conjugated secondary antibody (Dako, Glostrup, Denmark). Nuclei were counterstained with hematoxylin. Sections were examined with a Leica DC100 microscope (Leica Microsystems GmbH, Wetzlar, Germany; 10 x ocular lens, 20 x objective).

All animal care and experimental procedures were approved by the Bio-Ethical Committee of the University of Torino, Italy.

PCR arrays and qRT-PCR. Total RNA was extracted and reverse-transcribed using iScript™ cDNA Synthesis Kit (Bio-Rad Laboratories). The PCR arrays were performed on 1 μg cDNA, using Mitochondria and Mitochondria Energy Metabolism Arrays (Bio-Rad Laboratories). The expression levels of specific mitochondria-related genes, representative of the main biological categories screened by PCR arrays, were validated by qRT-PCR. Primer sequences were designed using qPrimerDepot software (https://primerdepot.nci.nih.gov/). *S14* was used as the housekeeping gene. Data analysis was performed with PrimePCR™ Analysis Software (Bio-Rad Laboratories).

Mitochondrial DNA quantification. Mitochondrial DNA was extracted, amplified and quantified by PicoGreen (Invitrogen Life Technologies) staining as reported in (19). The results are expressed as ng DNA/10^5 cells.

Mitochondria biogenesis. The expression of peroxisome proliferator-activated receptor gamma coactivator-1α (PGC-1α), measured on 30 μg of nuclear proteins and considered an index of increased mitochondria biogenesis (29), was evaluated by Western blotting, using an anti-PGC-1α (#ab54481; Abcam) antibody. An anti-TATA-box binding protein (TBP; clone 58C9; Santa Cruz Biotechnology Inc.) was used to check equal protein loading. Mitochondria biogenesis was also

evaluated by measuring the expressions of subunit I of complex IV (COX-I), which is encoded by mitochondrial DNA, and succinate dehydrogenase-A of complex II (SDH-A), which is encoded by nuclear DNA, using the MitoBiogenesis™ In-Cell ELISA Kit (Abcam). The results are expressed as units (U) of each protein/mg mitochondrial proteins.

Tricarboxylic acid (TCA) cycle. The glucose flux through TCA cycle was measured by radiolabeling cells with 2 μCi/mL [6-^{14}C]-glucose (55 mCi/mmol; PerkinElmer, Waltham, MA). Cell suspensions were incubated for 1 h in a closed experimental system to trap the $^{14}CO_2$ developed from[^{14}C]-glucose. The reaction was stopped by injecting 0.8 N $HClO_4$. The amount of glucose transformed into CO_2 through the TCA cycle was calculated as described by Riganti *et alia* (30) and expressed as pmol CO_2/h/mg cellular proteins.

Fatty acids β-oxidation. Long-chain fatty acids β-oxidation was measured as detailed in (31). The precipitates, containing ^{14}C-acid soluble metabolites (ASM), were collected. The radioactivity of each sample was counted by liquid scintillation. Results are expressed as pmol ASM. In each experimental set, cells were pre-incubated for 30 min with the carnitine palmitoyltransferase inhibitor etomoxir (1 μmol/L) or with the AMP-kinase activator 5-aminoimidazole-4-carboxamide ribonucleotide (AICAR; 1 mmol/L), as negative and positive controls, respectively. In the presence of etoxomir the rate of β-oxidation was less than 10% than in its absence; in the presence of AICAR, the rate of β-oxidation was increased two-fold.

Mitochondrial energy metabolism. The oxygen consumption rate (OCR) was measured on 20,000 cells with the XFp Mito Stress Test Kit, using a Seahorse XFp Extracellular Flux Analyzer (Seahorse Bioscience, M&M Biotech, Naples, Italy). Carbonyl cyanide 4-(trifluoromethoxy) phenylhydrazone (FCCP) was used at a concentration of 0.3 μmol/L to uncouple mitochondrial oxidative phosphorylation and induce maximal respiration. The data were analyzed using Wave Seahorse software. The amount of ATP produced by oxidative phosphorylation was measured on 20 μg mitochondrial proteins with the ATP Bioluminescent Assay Kit (FL-AA, Sigma Chemical Co.). Data were converted into nmol/mg mitochondrial proteins, using a previously set calibration curve.

Intramitochondrial reactive oxygen species (ROS) levels. After extraction, mitochondria were incubated with the ROS-sensitive probe 5-(and-6)-chloromethyl-2',7'-dichlorodihydro-fluorescein diacetate-acetoxymethyl ester (5 μmol/L; DCFDA-AM), as described (32).The results are expressed as nmol/mg mitochondrial proteins.

Mitochondrial electric potential (Δψ) measurement. Staining with a JC-1 fluorescent probe (Biotium Inc., Hayward, CA), was performed (32). The fluorescence units were used to calculate the percentage of green-fluorescent (i.e. depolarized) mitochondria versus red-fluorescent (i.e. polarized) mitochondria.

Apoptosis measurement. 20 μg proteins of whole cell, cytosolic or mitochondrial extracts were subjected to the Western blot analysis with the following antibodies (all from Cell Signaling Technology, Danvers, MA): anti-BAD (clone 11E3); anti-BAK (clone D4E4); anti-BAX (#2772); anti-BID (#2002); anti-BIM (clone C34C5); anti-PUMA (clone D30C10); anti-BCL-2 (#2872); anti-BCL-xL (clone #2762); anti-cytochrome c (#4272). Images were acquired by Image Lab^{TM} software (Bio-Rad Laboratories). Caspase 9 and caspase 3 activity was measured fluorimetrically in the cytosolic extracts (17).The results are expressed as nmol of the hydrolyzed substrate of each caspase/mg cellular proteins, according to a previously set titration curve.

Statistical analysis. All data in the text and figures are provided as means $\pm$ SD. The results were analyzed by a one-way analysis of variance (ANOVA) and Tukey's test. $p < 0.05$ was considered significant.

Results

Mitochondria-targeted doxorubicin is effective against doxorubicin-resistant osteosarcoma

We compared the anti-tumor efficacy of Dox and mtDox in the Dox-sensitive human osteosarcoma U-2OS cells and in the corresponding Dox-resistant variants U-2OS/DX30, U-2OS/DX100, U-2OS/DX580, with increasing expression of Pgp and MRP1 (Supplementary Figure S2). Dox exhibited typical nuclear localization in U-2OS cells (Figure 1A). There was a high accumulation of the drug in the nuclear extracts (Figure 1B) and a low accumulation in mitochondria (Figure 1C) in

U-2OS cells, while both nuclear and mitochondrial accumulation progressively decreased in U-2OS/DX30, U-2OS/DX100 and U-2OS/DX580 cells. By contrast, mtDox had a distinct mitochondrial localization profile in U-2OS cells (Figure 1A): intranuclear accumulation was very low in both sensitive and resistant cells (Figure 1B); intramitochondrial accumulation was significantly higher than Dox and progressively increased in the resistant cells (Figure 1C). At a concentration (5 μmol/L) corresponding to the IC_{50} in chemosensitive osteosarcoma (Supplementary Table S1), Dox retention in the whole cell was progressively lower (Figure 1D) and the inhibition of cell survival was lost (Figure 1E) in the resistant variants. However, at the same concentration, mtDox exhibited lower intracellular accumulation in the most resistant variants (Figure 1D), but it still reduced cell survival (Figure 1E).

Dox is one of the few chemotherapeutic drugs able to induce direct cytotoxicity on tumor cells, as indicated by the extracellular release of LDH (26). It is also able to elicit tumor immunogenic cell death, typically followed by tracking the by the extracellular release of ATP and HMGB1, and by monitoring cell surface levels of the immune-activating protein calreticulin (33). In U-2OS cells, Dox increased the extracellular release of LDH (Figure 1F), ATP (Figure 1G) and HMGB1 (Figure 1H), and surface expression of calreticulin (Figure 1I), but it progressively lost these properties in the resistant variants. By contrast, mtDox increased all these parameters in sensitive and resistant cells (Figure 1F-I).

The effects of mtDox were not cell line- or species-specific. Indeed, mtDox exhibited greater intracellular accumulation and was more cytotoxic than Dox in human Saos-2 cells and the corresponding resistant variants Saos-2/DX30, Saos-2/DX100, Saos-2/DX580 cells (Supplementary Figure S3A-B; Supplementary Table S1), as well as in murine Pgp-expressing K7M2 cells (Supplementary Figure S3C-E; Supplementary Table S1). However, mtDox exhibited lower intracellular accumulation (Supplementary Figure S4A, 4D) and was less toxic (Supplementary Figure S4B-C, S4E-F), in non-transformed osteoblasts and H9c2 cardiomyocytes, where it had a higher IC_{50} than Dox (Supplementary Table S1).

K7M2 tumors implanted in immunocompetent BALB/c mice did not respond to the maximum tolerated dose (MTD, 5 mg/kg) of Dox (Figure 2A-C). Dox neither reduced K7M2 cell proliferation (Figure 2D), nor increased the activity of caspase 3 (Figure 2E), the amount of surface calreticulin (Figure 2F), the tumor cell phagocytosis by DCs (Figure 2G). On the contrary, mtDox elicited all these effects (Figure 2). Immuhistochemical staining of K7M2 tumor sections confirmed that mtDox reduced tumor cell proliferation, increased apoptotic and calreticulin-positive cells, and increased intratumor infiltration of DCs (Supplementary Figure S5). According to the hematochemical parameters of the animals at the time of sacrifice, mtDox was significantly less cardiotoxic than Dox and did not elicit liver or kidney toxicity (Table 1). Dose-response experiments revealed that the anti-tumor effect of mtDox was dose-dependent and that the drug was still effective against resistant osteosarcoma at 1/5 of Dox MTD (Supplementary Figure S6). By contrast, mtDox did not produce any significant advantage compared to Dox against drug-sensitive tumors (Supplementary Figure S7).

Mitochondria-targeting doxorubicin deeply alters the expression of mitochondria-related genes in doxorubicin-resistant osteosarcoma cells

We next analyzed the expression of genes involved in mitochondria functions and mitochondria-dependent apoptosis. As shown in Figure 3A and Supplementary Table S2, the progressive increase in Dox resistance was paralleled by the upregulation of genes controlling processing, import and folding of mitochondrial proteins; mitochondrial fusion, fission and trafficking; transport of metabolites and co-factors across the mitochondrial membranes; mitochondrial metabolic pathways, such as TCA cycle, fatty acids β-oxidation and electron transport; ATP synthesis; ROS protection, such as superoxide dismutase (*SOD*) 1 and 2. However, genes encoding for proteins uncoupling oxidative phosphorylation and ATP synthesis, such as *SLC25A27* and *UCP1*, were progressively downregulated.

In drug-sensitive U-2OS cells, both Dox and mtDox downregulated at least two-fold 25 genes encoding for metabolite transporters, subunits of respiratory chain complexes and ATP synthase,

anti-oxidant genes such as *SOD1* and *SOD2*, and anti-apoptotic genes such as *BCL2* and *BCL2L1* (also known as *Bcl-xL*). They both upregulated genes encoding for the uncoupling proteins SLC25A27, UCP1, UCP2, UCP3 as well as the pro-apoptotic genes *BAK1*, *BBC3* (also known as *PUMA*), and *BNIP3* (Figure 3B; Supplementary Table S3). In U-2OS/DX580 cells, Dox up- or downregulated most of these genes less than one-fold, consistently with the low drug accumulation and efficacy. MtDox, by contrast, downregulated at least two-fold the vast majority of genes involved in protein import and processing, mitochondrial fusion and fission, metabolite and electron transport, ATP synthesis, ROS protection, and apoptosis inhibition. In parallel, mtDox upregulated genes encoding for uncoupling proteins (e.g. *SLC25A27*, *UCP1* and *UCP3*) and pro-apoptotic factors (e.g. *BAK1*, *BBC3*, *BID*, *BNIP3*; Figure 3C; Supplementary Table S4).

Given the distinct signatures of drug-sensitive versus drug-resistant variants and the diverse effects of Dox versus mtDox in resistant cells, we then investigated the impact of mtDox on mitochondria biogenesis and energy metabolism in our osteosarcoma models. Up- or down-regulation of key mitochondria-related genes were validated by qRT-PCR (Supplementary Tables S5-S7). For the sake of simplicity, we only show the results obtained in U-2OS and U-2OS/DX580 cells. The effects of Dox and mtDox on gene expression and the mitochondrial functions of U-2OS/DX30 and U-2OS/DX100 variants were intermediate relative to those produced in U-2OS and U-2OS/DX580 cells.

Mitochondria-targeted doxorubicin reduces mitochondrial biogenesis, protein import and energy metabolism in doxorubicin-resistant osteosarcoma cells

Compared to U-2OS cells, U-2OS/DX580 cells had higher mitochondrial DNA (Figure 4A) and protein content (Figure 4B), a higher level of nuclear translocation of PGC-1α (Figure 4C) and higher expression of COX-I (Figure 4D), which is encoded by mitochondrial DNA. These observations are consistent with increased mitochondria biogenesis in the resistant variant. SDH-A, which is encoded by nuclear DNA, was also higher (Figure 4E), likely in consequence of the higher expression of mitochondrial protein importers in U-2OS/DX580 cells. Consistent with the gene

expression signature, U-2OS/DX580 cells had elevated: TCA cycle (Figure 4F); fatty acids β-oxidation rate (Figure 4G); ATP-linked OCR (Figure 4H, 4I); maximal respiration capacity (Figure 4H, 4J), and ATP synthesis by oxidative phosphorylation (Figure 4K). Dox and mtDox decreased all these parameters in drug-sensitive cells. Only mtDox affected these pathways in drug-resistant cells (Figure 4).

Mitochondria-targeting doxorubicin triggers a mitochondria-dependent apoptosis in drug-resistant osteosarcoma cells

We did not detect any significant differences in intramitochondrial ROS levels in U-2OS and U-2OS/DX580 cells (Figure 5A). Dox increased ROS in drug-sensitive cells but not in drug-resistant ones; mtDox significantly increased intramitochondrial ROS in both cell populations (Figure 5A). The higher levels of ROS were paralleled by mitochondrial depolarization (Figure 5B). Dox increased pro-apoptotic proteins such as BAK, active BID (tBID) and PUMA, and decreased anti-apoptotic proteins such as BCL-2 and BCL-xL only in U-2OS cells. mtDox elicited these effects in both variants (Figure 5C), in line with its effects on gene expression. Consistent with the change in mitochondria polarization, Dox increased mitochondria-associated Bad, Bak, Bax, tBid, Bim_L and Puma, the release of cytochrome c into the cytosol (Figure 5D), the activity of caspase 9 (Figure 5E) and caspase 3 (Figure 5F) only in drug-sensitive cells, whereas mtDox produced these effects in both U-2OS and U-2OS/DX580 cells (Figure 5D-F).

Discussion

Since targeting mitochondria is an effective therapeutic strategy in osteosarcoma (16), we used chemically-modified Dox with a mitochondrial tropism against Dox-sensitive and Dox-resistant osteosarcoma cells. This modified mtDox was effective against osteosarcoma cells overexpressing Pgp and showing resistance to Dox.

The selective delivery into the mitochondria, due to the conjugation of the anthracycline moiety with a peptide containing cationic and hydrophobic residues that deliver cargoes into mitochondria (34), may limit the availability of Dox for the Pgp on the plasma membrane, reducing the efflux of

the drug from tumor cells (18). Our work supports this hypothesis: unlike Dox, mtDox was well retained within mitochondria in both drug-sensitive and drug-resistant/Pgp-overexpressing osteosarcoma cells. While Dox accumulation and cytotoxic efficacy dramatically decreased in the Pgp-overexpressing variants, mtDox accumulation within resistant cells was only slightly lower and its cytotoxicity remained high in Pgp-overexpressing cells. While these data might suggest that Pgp effluxes both mtDox and Dox, the preferential intramitochondrial delivery of the former preserves its high intracellular retention.

The higher the intracellular accumulation of Dox, the higher the ability of the drug to kill cancer cells due to the induction of necro-apoptotic death and activation of the host immune system against the tumor (35): Dox promotes the exposure on the plasma membrane of calreticulin, which activates the local DCs to phagocytize tumor cells, stimulating a subsequent expansion of anti-tumor $CD8^+$ T-lymphocytes and eliciting a durable anti-tumor response (36). These mechanisms do not work in drug-resistant tumors (35). Neither cytotoxic nor pro-immunogenic effects were exerted by Dox in Pgp-overexpressing osteosarcoma cells. MtDox, however, exerted all the canonical effects of anthracyclines in drug-resistant cells as well, as suggested by the extracellular release of LDH and by the increase of immunogenic cell death biomarkers (extracellular ATP and HMGB1 release, surface calreticulin). Mitochondrial depolarization, changes in calcium homeostasis and increased ROS levels have been correlated with calreticulin upregulation and translocation from endoplasmic reticulum (ER) to the plasma-membrane (37, 38): indeed, changes in intramitochondrial calcium and ROS are “sensed” by the ER-membrane-associated to mitochondria (MAM) compartment, which is rich in calreticulin and controls the protein trafficking to the plasma membrane (39). Since mtDox depolarized mitochondria and increased ROS in both drug-sensitive and drug-resistant osteosarcoma cells, these events likely trigger the upregulation of calreticulin and/or its translocation from ER/MAM to the plasma-membrane.

The efficacy of mtDox was validated in a pre-clinical model of Dox-resistant osteosarcoma implanted in immunocompetent animals, i.e. the Pgp-expressing K7M2 cells that are syngeneic

with BALB/c mice. In both *in vitro* and *in vivo* assays, mtDox exerted direct cytotoxicity on tumor cells (as indicated by the reduced tumor growth and cell proliferation, and by the increased apoptosis) and primed tumor cells for the recognition by the host immune system (as suggested by the increased percentage of calreticulin-positive tumor cells, tumor cell phagocytosis and intratumor DC infiltration). Moreover, mtDox still retained anti-tumor efficacy at 1/2-1/5 of Dox MTD. Importantly, unlike the mice treated with Dox, those treated with mtDox did not show any increase in CPK. These results are in accordance with previous observations, showing that mtDox did not exert systemic and cardio-specific toxicity *in vivo* (19), and with the reduced toxicity observed in cultured cardiomyocytes. In preclinical models, mtDox was more advantageous than Dox in drug-resistant tumors, not in drug-sensitive ones, leading to hypothesize that the greater efficacy of mtDox was due to the targeting of pathways which are crucial for the survival of drug-resistant cells.

The increase of Dox resistance was associated with the upregulation of genes controlling mitochondrial biogenesis, the import of proteins, metabolites and co-factors, and energy metabolism, and with the downregulation of genes encoding for uncoupling proteins. This signature made the mitochondria metabolism of Dox-resistant osteosarcoma cells more efficient, as confirmed by the higher content of mitochondrial DNA and proteins, and by the higher metabolic flux through the main energy pathways in U-2OS/DX580 cells. It is noteworthy that genes encoded by both nuclear and mitochondrial DNA were upregulated in drug-resistant cells. These results suggest that the higher mitochondrial metabolism of drug-resistant cells was supported partly by the increased mitochondria biogenesis and partly by the increased import of cytosolic proteins and metabolites within mitochondria. This process may favor a more efficient assembly of mitochondrial complexes involved in the TCA cycle, fatty acids β-oxidation, electron transport and ATP synthesis, and may supply all these pathways with anaplerotic metabolites and essential co-factors. Contrarily to most tumor cells, which obtain energy from anaerobic glycolysis, chemoresistant cells often simultaneously activate glycolysis and oxidative phosphorylation to meet

their energy requirements (40). The higher ATP level produced by mitochondrial oxidative phosphorylation may support the ATP-dependent efflux activity of ABC transporters, contributing to the chemoresistant phenotype. On the other hand, a high proton motive force induces a high production of ROS from mitochondria (41). We did not detect any differences in intramitochondrial ROS between U-2OS and U-2OS/DX580 cells, which was most likely due to the upregulation of mitochondrial *SOD2* in the latter: this feature may also contribute to chemoresistance.

Dox acts through pleiotropic mechanisms on tumor cells, including mitochondrial-dependent mechanisms. For example,it reduces the activity of complexes I, II and III (42) and the synthesis of ATP (43), and increases intramitochondrial ROS through iron-catalyzed redox cycles within complex I (44). In sensitive osteosarcoma cells, Dox downregulated specific metabolite transporters, subunits of mitochondrial respiratory complexes and ATP synthase, cytosolic and mitochondrial isoforms of *SOD*, and upregulated uncoupling proteins and pro-apoptotic factors. The consequent reduction of mitochondria biogenesis and ATP synthesis, coupled with the increase in intramitochondrial ROS, triggered a mitotoxicity-dependent apoptosis. None of these events occurred in the drug-resistant U-2OS/DX580 variant, where Dox did not reach an intracellular concentration sufficient to elicit effects at genomic and metabolic levels.

By contrast, mtDox produced genomic and metabolic signatures that were similar in drug-sensitive and drug-resistant osteosarcoma cells. By downregulating genes involved in mitochondria biogenesis and mitochondrial protein import, it significantly reduced mitochondrial DNA and protein contents. Previously, it was reported that in cardiomyocytes mtDox decreased mitochondrial DNA after 6 h and increased it after 24 h: this trend suggests a recovery from the initial damage due to mitochondrial biogenesis. On the contrary, in ovarian cancer cells mitochondrial DNA levels remained significantly lower after 24 h of treatment with mtDox, indicating that tumor cells are not able to increase mitochondrial biogenesis in response to mtDox (19). These findings are in line with the results obtained in osteosarcoma cells. The different response of cardiomyocytes and tumor cells

to the mitochondrial damage elicited by mtDox may explain the key properties of mtDox, i.e. its anti-tumor efficacy and its cardiac safety.

By decreasing the expression of several transporters and subunits of oxidative phosphorylation complexes, mtDox strongly reduced the mitochondrial energy metabolism. It is noteworthy that it upregulated the expression of uncoupling proteins and pro-apoptotic factors, and markedly decreased the expression of mitochondrial *SOD2*. These events uncoupled oxidative phosphorylation from ATP synthesis and increased the intramitochondrial levels of ROS, which were not buffered by SOD2. This metabolic dysfunction causes the opening of the mitochondrial permeability transition pore and triggers a downregulation of mitochondria-dependent apoptosis. The simultaneous downregulation of anti-apoptotic genes further supported the apoptotic process. The events described above were more pronounced in Dox-resistant cells than in Dox-sensitive ones, in accordance with the higher mitochondrial metabolic activity of the former. Of note, mtDox was relatively non-toxic in non-transformed osteoblasts. On one hand, the lower uptake of mtDox by non-transformed cells may explain the reduced toxicity; on the other hand, osteoblasts are more dependent on anaerobic glycolysis than on mitochondrial metabolism for their growth and differentiation (45, 46). These factors may explain the relatively selective cytotoxicity of mtDox for tumor cells over non-transformed cells.

Despite their resistance to chemotherapy, drug-resistant tumors are more susceptible than drug-sensitive ones to the depletion of ATP and to the increase of ROS, an event known as “collateral sensitivity” (CS) (47). Agents that lower intracellular ATP and/or increase ROS levels are effective against chemoresistant cells *in vitro*. Unfortunately, the intrinsic toxicity of these agents limits their use *in vivo* (48). However, thanks to its ability to lower the levels of ATP produced by oxidative phosphorylation and increase ROS levels within drug-resistant cells, mtDox is an excellent inducer of CS. Unlike the other compounds exerting CS, it did not produce appreciable toxicity for the liver, kidneys or heart in our pre-clinical model of resistant osteosarcoma, thus appearing suitable for being used *in vivo*.

The novelty of the therapeutic strategy proposed in this work relates to two factors. First, we used a derivative of a first-line drug Dox, the efficacy of which is limited by the expression of Pgp in osteosarcoma cells and by the development of cardiotoxicity: by chemically modifying Dox to achieve its selective delivery into mitochondria, we overcame a key limitation frequently encountered in patients treated with Dox-based regimens. Second, mtDox exploited a metabolic signature typical of chemoresistant cells - i.e. the hyperactive mitochondrial metabolism - and hit energy pathways that are crucial for drug-resistant tumors. This drug conjugate produced promising results that that may be applied to the treatment of Pgp-expressing osteosarcomas. These results may pave the way for the potential use of mtDox in clinical settings, in particular for patients with Pgp-positive osteosarcomas or as a possible second-line treatment for relapsed patients.

Acknowledgments

We are grateful to Prof. Amalia Bosia, Department of Oncology, University of Torino, for the fruitful discussion, and to Dr. Erika Ortolan, Department of Medical Sciences, University of Torino, for technical assistance. We are also grateful to Mr. Andrew Martin Garvey, BAHons LTCL(TESOL) PGDip MA, for editorial assistance.

References

1. Rivera-Valentin RK, Zhu L, Hughes DP. Bone Sarcomas in Pediatrics: Progress in Our Understanding of Tumor Biology and Implications for Therapy. Paediatr Drugs 2015;17:257–71.
2. Hattinger CM, Fanelli M, Tavanti E, Vella S, Ferrari S, Picci P, et al. Advances in emerging drugs for osteosarcoma. Expert Opin Emerg Drugs 2015;20:495–514.
3. Lipshultz SE, Karnik R, Sambatakos P, Franco VI, Ross SW, Miller TL. Anthracycline-related cardiotoxicity in childhood cancer survivors. Curr Opin Cardiol 2014;29:103–12.
4. Gottesman MM, Fojo T, Bates SE. Multidrug resistance in cancer: role of ATP-dependent transporters. Nat Rev Cancer 2002;2:48–58.
5. Baldini N, Scotlandi K, Barbanti-Bròdano G, Manara MC, Maurici D, Bacci G, et al. Expression of P-glycoprotein in high-grade osteosarcomas in relation to clinical outcome. N Engl J Med 1995;333:1380–85.
6. Serra M, Scotlandi K, Reverter-Branchat G, Ferrari S, Manara MC, Benini S, et al. Value of P-glycoprotein and clinicopathologic factors as the basis for new treatment strategies in high-grade osteosarcoma of the extremities. J Clin Oncol 2003;21:536–42.
7. Serra M, Pasello M, Manara MC, Scotlandi K, Ferrari S, Bertoni F, et al. May P-glycoprotein status be used to stratify high-grade osteosarcoma patients? Results from the Italian/Scandinavian Sarcoma Group 1 treatment protocol. Int J Oncol 2006;29:1459–68.
8. Bramer JA, van Linge JH, Grimer RJ, Scholten RJ. Prognostic factors in localized extremity osteosarcoma: a systematic review. Eur J Surg Oncol 2009;35:1030–36.
9. Condello M, Cosentino D, Corinti S, Di Felice G, Multari G, Gallo FR, et al. Voacamine modulates the sensitivity to doxorubicin of resistant osteosarcoma and melanoma cells and does not induce toxicity in normal fibroblasts. J Nat Prod 2014;77:855–62.

10. Xia YZ, Ni K, Guo C, Zhang C, Geng YD, Wang ZD, et al. Alopecurone B reverses doxorubicin-resistant human osteosarcoma cell line by inhibiting P-glycoprotein and NF-kappa B signaling. Phytomedicine 2015;22:344–51.
11. Duan Z, Zhang J, Ye S, Shen J, Choy E, Cote G, et al. A-770041 reverses paclitaxel and doxorubicin resistance in osteosarcoma cells. BMC Cancer 2014;14:e681.
12. Yang X, Yang P, Shen J, Osaka E, Choy E, Cote G, et al. Prevention of multidrug resistance (MDR) in osteosarcoma by NSC23925. Br J Cancer 2014;110:2896–904.
13. Susa M, Iyer AK, Ryu K, Choy E, Hornicek FJ, Mankin H, et al. Inhibition of ABCB1 (MDR1) expression by an siRNA nanoparticulate delivery system to overcome drug resistance in osteosarcoma. PLoS One 2010;5:e10764.
14. Roncuzzi L, Pancotti F, Baldini N. Involvement of HIF-1α activation in the doxorubicin resistance of human osteosarcoma cells. Oncol Rep 2014;32:389–94.
15. Sero V, Tavanti E, Vella S, Hattinger CM, Fanelli M, Michelacci F, et al. Targeting polo-like kinase 1 by NMS-P937 in osteosarcoma cell lines inhibits tumor cell growth and partially overcomes drug resistance. Invest New Drugs 2014;32:1167–80.
16. Armstrong J, Dass CR. Doxorubicin action on mitochondria: relevance to osteosarcoma therapy? Curr Drug Targets 2015, in press.
17. Riganti C, Rolando B, Kopecka J, Campia I, Chegaev K, Lazzarato L, et al. Mitochondrial-targeting nitrooxy-doxorubicin: a new approach to overcome drug resistance. Mol Pharm 2013;10:161–74.
18. Chamberlain GR, Tulumello DV, Kelley SO. Targeted delivery of doxorubicin to mitochondria. ACS Chem Biol 2013;8:1389–95.
19. Jean SR, Tulumello DV, Riganti C, Liyanage SU, Schimmer AD, Kelley SO. Mitochondrial Targeting of Doxorubicin Eliminates Nuclear Effects Associated with Cardiotoxicity. ACS Chem Biol 2015;10:2007-15.

20. Serra M, Scotlandi K, Manara MC, Maurici D, Lollini PL, De Giovanni C, et al. Establishment and characterization of multidrug-resistant human osteosarcoma cell lines. Anticancer Res 1993;13:323–29.

21. Gronthos S, Zannettino AC, Hay SJ, Shi S, Graves SE, Kortesidis A, et al. Molecular and cellular characterisation of highly purified stromal stem cells derived from human bone marrow. J Cell Sci 2003;116:1827-35.

22. Brunetti G, Rizzi R, Oranger A, Gigante I, Mori G, Taurino G, et al. LIGHT/TNFSF14 increases osteoclastogenesis and decreases osteoblastogenesis in multiple myeloma-bone disease. Oncotarget 2014;5:12950-67.

23. Gelsomino G, Corsetto PA, Campia I, Montorfano G, Kopecka J, Castella B, et al. Omega 3 fatty acids chemosensitize multidrug resistant colon cancer cells by downregulating cholesterol synthesis and altering detergent resistant membranes composition. Mol Cancer 2013;12:e137.

24. Riganti C, Salaroglio IC, Caldera V, Campia I, Kopecka J, Mellai M, et al. Temozolomide downregulates P-glycoprotein expression in glioblastoma stem cells by interfering with the Wnt3a/GSK3/β-catenin pathway. Neuro-Oncol 2013;15:1502–17.

25. Campia I, Lussiana C, Pescarmona G, Ghigo D, Bosia A, Riganti C. Geranylgeraniol prevents the cytotoxic effects of mevastatin in THP-1 cells, without decreasing the beneficial effects on cholesterol synthesis. Br J Pharmacol 2009;158:1777–86.

26. Riganti C, Miraglia E, Viarisio D, Costamagna C, Pescarmona G, Ghigo D, et al. Nitric oxide reverts the resistance to doxorubicin in human colon cancer cells by inhibiting the drug efflux. Cancer Res 2005;65:516–25.

27. Riganti C, Castella B, Kopecka J, Campia I, Coscia M, Pescarmona G, et al. Zoledronic acid restores doxorubicin chemosensitivity and immunogenic cell death in multidrug-resistant human cancer cells. PLoS One 2013;8:e60975.

28. Obeid M, Tesniere A, Ghiringhelli F, Fimia GM, Apetoh L, Perfettini JL, et al. Calreticulin exposure dictates the immunogenicity of cancer cell death. Nat Med 2007; 13:54–61.

29. LeBleu VS, O'Connell JT, Gonzalez Herrera KN, Wikman H, Pantel K, Haigis MC, et al. PGC-1α mediates mitochondrial biogenesis and oxidative phosphorylation in cancer cells to promote metastasis. Nat Cell Biol 2014;16:992–1003.

30. Riganti C, Gazzano E, Polimeni M, Costamagna C, Bosia A, Ghigo D. Diphenyleneiodonium inhibits the cell redox metabolism and induces oxidative stress. J Biol Chem 2004;279:47726–31.

31. Gaster M, Rustan AC, Aas V, Beck-Nielsen H. Reduced Lipid Oxidation in Skeletal Muscle From Type 2 Diabetic Subjects May Be of Genetic Origin Evidence From Cultured Myotubes. Diabetes 2004;53:542–48.

32. Riganti C, Gazzano E, Gulino GR, Volante M, Ghigo D, Kopecka J. Two repeated low doses of doxorubicin are more effective than a single high dose against tumors overexpressing P-glycoprotein. Cancer Lett 2015;360:219–26.

33. Kepp O, Senovilla L, Vitale I, Vacchelli E, Adjemian S, Agostinis P, et al. Consensus guidelines for the detection of immunogenic cell death. Oncoimmunology 2014;3:e955691

34. Horton KL, Stewart KM, Foseca SB, Guo Q, Kelley SO. Mitochondria-penetrating peptides. Chem Biol 2008;15: 375–82.

35. De Boo S, Kopecka J, Brusa D, Gazzano E, Matera L, Ghigo D, et al. iNOS activity is necessary for the cytotoxic and immunogenic effects of doxorubicin in human colon cancer cells. Mol Cancer 2009;8:e108.

36. Apetoh L, Mignot G, Panaretakis T, Kroemer G, Zitvogel L. Immunogenicity of anthracyclines: moving towards more personalized medicine. Trends Mol Med 2008;14:141–51.

37. Biswas G, Guha M, Avadhani NG. Mitochondria-to-nucleus stress signaling in mammalian cells: nature of nuclear gene targets, transcription regulation, and induced resistance to apoptosis. Gene 2005;354:132–39.

38. Zhang Y, Liu L, Jin L, Yi X, Dang E, Yang Y, et al. Oxidative stress-induced calreticulin expression and translocation: new insights into the destruction of melanocytes. J Invest Dermatol 2014;134:183–91.

39. Poston CN, Krishnan SC, Bazemore-Walker CR. In-depth proteomic analysis of mammalian mitochondria-associated membranes (MAM). J Proteomics 2013;79:219–30.

40. Martinez-Outschoorn UE, Pestell RG, Howell A, Tykocinski ML, Nagajyothi F, Machado FS, et al. Energy transfer in "parasitic" cancer metabolism: mitochondria are the powerhouse and Achilles' heel of tumor cells. Cell Cycle 2011;10:4208–16.

41. Mailloux RJ, Harper ME. Mitochondrial proticity and ROS signaling: lessons from the uncoupling proteins. Trends Endocrinol Metab 2012;23:451–58.

42. Marcillat O, Zhang Y, Davies KJ. Oxidative and non-oxidative mechanisms in the inactivation of cardiac mitochondrial electron transport chain components by doxorubicin. Biochem J 1989;259:181–89.

43. Strigun A, Wahrheit J, Niklas J, Heinzle E, Noor F. Doxorubicin increases oxidative metabolism in HL-1 cardiomyocytes as shown by 13C metabolic flux analysis. Toxicol Sci 2012;125:595–606.

44. Simunek T, Sterba M, Popelova O, Adamcova M, Hrdina R, Gersl V. Anthracycline-induced cardiotoxicity: overview of studies examining the roles of oxidative stress and free cellular iron. Pharmacol Rep 2009;61:154–71.

45. Esen E, Chen J, Karner CM, Okunade AL, Patterson BW, Long F. WNT-LRP5 signaling induces Warburg effect through mTORC2 activation during osteoblast differentiation. Cell Metab 2013;17:745–55.

46. Regan JN, Lim J, Shi Y, Joeng KS, Arbeit JM, Shohet RV, et al. Upregulation of glycolytic metabolism is required for HIF1α-driven bone formation. Proc Natl Acad Sci USA 2014;111:8673–78.

47. Pluchino KM, Hall MD, Goldsborough AS, Callaghan R, Gottesman MM. Collateral sensitivity as a strategy against cancer multidrug resistance. Drug Resist Updat 2012;15:98–105.

48. Callaghan R, Luk F, Bebawy M. Inhibition of the multidrug resistance P-glycoprotein: time for a change of strategy? Drug Metab Dispos 2014;42:623–31.

Tables

Table 1. Hematochemical parameters of animals

	Ctrl	Dox	mtDox
LDH (U/L)	6231 ± 1098	6234 ± 724	6198 ± 821
AST (U/L)	187 ± 52	234 ± 27	212 ± 82
ALT (U/L)	38 ± 9	41 ± 5	43 ± 10
AP (U/L)	87 ± 13	94 ± 15	91 ± 13
Creatinine (mg/L)	0.041 ± 0.006	0.039 ± 0.008	0.037 ± 0.009
CPK (U/L)	321 ± 93	850 ± 150 *	453 ± 83

Animals (n = 10/group) were treated as reported under Materials and methods. Blood was collected immediately after mice euthanasia and analyzed for lactate dehydrogenase (LDH), aspartate aminotransferase (AST), alanine aminotransferase (ALT), alkaline phosphatase (AP), creatinine, creatine phosphokinase (CPK). Ctrl: mice treated with saline solution; Dox: mice treated with doxorubicin; mtDox: mice treated with mitochondria-targeting doxorubicin. Versus Ctrl group: *p < 0.005; mtDox group versus Dox group: ° p < 0.01.

Figure legends

Figure 1. Mitochondria-targeted doxorubicin is more accumulated and more cytotoxic than doxorubicin in drug-resistant osteosarcoma cells

Dox-sensitive U-2OS cells and Dox-resistant variants (U-2OS/DX30, U-2OS/DX100, U-2OS/DX580) were incubated in the absence (Ctrl) or in the presence of 5 μmol/L Dox or mtDox for 6 h (panels A-D), 24 h (panels F-I) or 72 h (panel E). **A.** U-2OS cells were incubated for 24 h with the GFP-E1α pyruvate dehydrogenase expression vector to label mitochondria, then treated with Dox or mtDox. The intracellular localization of the drugs was analyzed by confocal microscopy. Bar: 10 μm. The micrographs are representative of 3 experiments with similar results. **B.** The amount of Dox was measured spectrofluorimetrically in nuclear extracts in duplicate. Data are presented as means $\pm$ SD (n= 3). Versus U-2OS cells: * $p < 0.001$; mtDox versus Dox: ° $p < 0.001$. **C.** The amount of Dox was measured spectrofluorimetrically in isolated mitochondria in duplicate. Data are presented as means $\pm$ SD (n= 3). Versus U-2OS cells: * $p < 0.02$; mtDox versus Dox: ° $p < 0.001$. **D.** The content of Dox in whole cell lysates was measured spectrofluorimetrically in duplicate. Data are presented as means $\pm$ SD (n= 4). Versus U-2OS cells: * $p < 0.05$; mtDox versus Dox: ° $p < 0.002$. **E.** Cells were stained with neutral red solution in quadruplicate. The results were expressed as a percentage of viable cells versus untreated cells. Data are presented as means $\pm$ SD (n= 3). Versus respective Ctrl: * $p < 0.001$; mtDox versus Dox: ° $p < 0.01$. **F**. The release of LDH in the extracellular medium was measured spectrophotometrically in duplicate. Data are presented as means $\pm$ SD (n= 4). Versus respective Ctrl: * $p < 0.005$; mtDox versus Dox: ° $p < 0.001$. **G.** The extracellular release of ATP was measured in duplicate by a chemiluminescence-based assay. Data are presented as means $\pm$ SD (n = 3). Versus respective Ctrl: * $p < 0.001$; mtDox versus Dox: ° $p < 0.001$. **H.** The release of HMGB1 in the cell supernatants was analyzed by Western blotting. Red Ponceau staining was used to check the equal loading of proteins. The figure is representative of 1 out of 3 experiments. **I.** The amount of surface calreticulin was measured by flow cytometry in

duplicate. Left panel: histograms representative of 3 experiments with similar results; right panel: mean fluorescence intensity (MFI) of calreticulin-positive cells. Data are presented as means ± SD (n = 3). Versus respective Ctrl: * $p < 0.01$; mtDox versus Dox: ° $p < 0.001$.

Figure 2. Mitochondria-targeted doxorubicin is effective against drug-resistant osteosarcoma *in vivo*

Six week-old female BALB/c mice were inoculated s.c. with 1 x 10^6 K7M2 cells. When the tumor reached the volume of 50 mm^3 (day 7), the animals (10 mice/group) were randomized and treated on days 7, 14, 21, 28 as follows: 1) Ctrl group, treated with 0.1 mL saline solution i.v.; 2) Dox group, treated with 5 mg/kg Dox i.v.; 3) mtDox group, treated with 5 mg/kg mitochondria-targeted Dox i.v. **A.** Representative *in vivo* bioluminescence imaging, performed on days 7, 21, 35 after implant. **B.** Tumor growth monitored by caliper measurements. Arrows represent saline, Dox or mtDox injections. Data are presented as means ± SD. Versus Ctrl group: * $p < 0.001$; mtDox group versus Dox group: ° $p < 0.001$. The inhibition rate in Dox-treated animals was 16.86%, in mtDox-treated animals it was 45.49%. **C.** Photographs of representative tumors from each treatment group after mice sacrifice. **D-G.** K7M2 cells were left untreated (Ctrl) or treated for 24 h with 5 μmol/L Dox or mtDox. **D.** Cell cycle analysis was measured by flow cytometry. Data are presented as means ± SD (n = 3). Versus Ctrl: * $p < 0.01$; mtDox versus Dox: ° $p < 0.001$. **E.** The activity of caspase 3 was measured fluorimetrically in duplicate in the cytosolic extracts. Data are presented as means ± SD (n = 4). Versus Ctrl: * $p < 0.001$; mtDox versus Dox: ° $p < 0.001$. **F.** The amount of surface calreticulin was measured by flow cytometry in duplicate. Left panel: histograms are representative of 1 out of 3 experiments; right panel: mean fluorescence intensity (MFI) of calreticulin-positive cells. Data are presented as means ± SD (n = 3). Versus Ctrl: * $p < 0.001$; mtDox versus Dox: ° $p < 0.001$. **G.** DC-mediated phagocytosis of K7M2 cells was measured by flow cytometry. Data are presented as means ± SD (n = 4). The phagocytic index of untreated cells was considered as 1. Versus Ctrl: * $p < 0.002$; mtDox versus Dox: ° $p < 0.005$.

Figure 3. Modulation of mitochondria-related genes by doxorubicin and mitochondria-targeted doxorubicin in drug-sensitive and drug-resistant osteosarcoma cells

A. The cDNA from Dox-sensitive U-2OS cells and Dox-resistant variants (U-2OS/DX30, U-2OS/DX100, U-2OS/DX580) was analyzed by PCR arrays specific for mitochondria-related genes, as reported under Materials and methods. The figure reports the genes up- or downregulated two-fold or more in at least one cell line, in a colorimetric scale (n = 4). **B-C.** U-2OS cells (panel **B**) or U-2OS/DX580 cells (panel **C**) were grown for 24 h in fresh medium (Ctrl), in medium containing 5 μmol/L Dox or mtDox. The cDNA was analyzed by the same PCR arrays of panel **A**. The figures report the genes up- or downregulated two-fold or more in at least one experimental condition, in a colorimetric scale (n = 4). OXPHOS: oxidative phosphorylation.

Figure 4. Mitochondria biogenesis and energy metabolism in cells treated with doxorubicin or mitochondria-targeted doxorubicin

Dox-sensitive U-2OS cells and Dox-resistant U-2OS/DX580 cells were incubated in the absence (Ctrl) or in the presence of 5 μmol/L Dox or mtDox for 24 h. Data are presented as means $\pm$ SD (n = 4). **A-B.** The amount of mitochondrial DNA (panel **A**) and proteins (panel **B**) was measured in duplicate after mitochondria isolation, as described under Materials and methods. For both panels, versus U-2OS Ctrl cells: * $p < 0.05$; versus U-2OS/DX580 Ctrl cells: ° $p < 0.02$; U-2OS/DX580 versus U-2OS cells: $^{\#}$ $p < 0.001$. **C.** Nuclear extracts were analyzed for the levels of PGC-1α by Western blotting. The TBP expression was used as the control of equal protein loading. The figure is representative of 1 out of 3 experiments. **D-E**. The expression of subunit I of complex IV (COX-I, panel **D**) and succinic acid dehydrogenase-A of complex II (SDH-A, panel **E**) was measured by quantitative immunocytochemistry in duplicate. For both panels, versus U-2OS Ctrl cells: * $p < 0.05$; versus U-2OS/DX580 Ctrl cells: ° $p < 0.001$; U-2OS/DX580 versus U-2OS cells: $^{\#}$ $p < 0.05$. **F.** The glucose flux through the TCA cycle was measured in duplicate in cells radiolabeled with [6-^{14}C]-glucose. Versus U-2OS Ctrl cells: * $p < 0.05$; versus U-2OS/DX580 Ctrl cells: ° $p < 0.001$; U-2OS/DX580 versus U-2OS cells: $^{\#}$ $p < 0.002$. **G.** The amount of ^{14}C-ASM derived from fatty acids

β-oxidation was measured in duplicate in cells labeled with [1-^{14}C]-palmitoyl coenzyme A. Versus U-2OS Ctrl cells: * $p < 0.001$; versus U-2OS/DX580 Ctrl cells: ° $p < 0.001$; U-2OS/DX580 versus U-2OS cells: $^{\#}$ $p < 0.05$. **H.** Mitochondrial bioenergetic profiles generated using the Seahorse XFp Analyzer, in U-2OS cells (left panel) and U-2OS/DX580 cells (right panel). The figures are representative of 1 out of 4 experiments, each performed in triplicate. **I-J.** ATP-linked OCR rates (panel **I)** and maximal respiration (panel **J**) were determined from the bioenergetic profiles of panel **H**. ATP-linked OCR represents the difference between basal and oligomycin-treated OCR, while maximal respiration represents the difference between FCCP- and rotenone/antimycin-treated OCR. Versus U-2OS Ctrl cells: * $p < 0.05$; versus U-2OS/DX580 Ctrl cells: ° $p < 0.001$; U-2OS/DX580 versus U-2OS cells: $^{\#}$ $p < 0.05$. **K.** ATP levels in isolated mitochondria were measured in duplicate by a chemiluminescence-based assay. Versus U-2OS Ctrl cells: * $p < 0.05$; versus U-2OS/DX580 Ctrl cells: ° $p < 0.005$; U-2OS/DX580 versus U-2OS cells: $^{\#}$ $p < 0.01$.

Figure 5. Effects of doxorubicin and mitochondria-targeted doxorubicin on mitochondria integrity and mitochondria-dependent apoptosis

Dox-sensitive U-2OS cells and Dox-resistant U-2OS/DX580 cells were incubated in the absence (Ctrl) or in the presence of 5 μmol/L Dox or mtDox for 24 h. **A.** Intramitochondrial ROS levels were measured fluorimetrically in triplicate using the DCFDA-AM probe. Data are presented as means $\pm$ SD (n = 4). Versus U-2OS Ctrl cells: * $p < 0.001$; versus U-2OS/DX580 Ctrl cells: ° $p < 0.001$; U-2OS/DX580 versus U-2OS cells: $^{\#}$ $p < 0.001$. **B.** The mitochondrial membrane potential was assessed in duplicate by the JC-1 staining method. The percentage of green versus red mitochondria was considered an index of mitochondrial depolarization and permeability transition. Data are presented as means $\pm$ SD (n = 4). Versus U-2OS Ctrl cells: * $p < 0.005$; versus U-2OS/DX580 Ctrl cells: ° $p < 0.005$; U-2OS/DX580 versus U-2OS cells: $^{\#}$ $p < 0.002$. **C.** Whole cell lysates were probed with the indicated antibodies. BID full-length and truncated (tBID) protein, BIM isoforms BIM_{EL}, BIM_L, BIM_S are shown. The β-tubulin expression was used as the control of equal protein loading. The figure is representative of 1 out of 3 experiments. **D.** Mitochondrial and

cytosolic extracts were subjected to Western blotting and probed with the indicated antibodies. tBID and BIM_L isoforms are shown. Porin and β-tubulin expression were used as the control of equal protein loading in the respective extracts. The figure is representative of 1 out of 3 experiments. **E-F.** The activity of caspase 9 (panel **E**) and caspase 3 (panel **F**) was measured fluorimetrically in duplicate in the cytosolic extracts. Data are presented as means $\pm$ SD (n = 4). For both panels, versus U-2OS Ctrl cells: * $p < 0.001$; versus U-2OS/DX580 Ctrl cells: ° $p < 0.001$; U-2OS/DX580 versus U-2OS cells: $^{\#}$ $p < 0.001$.

Figure 1

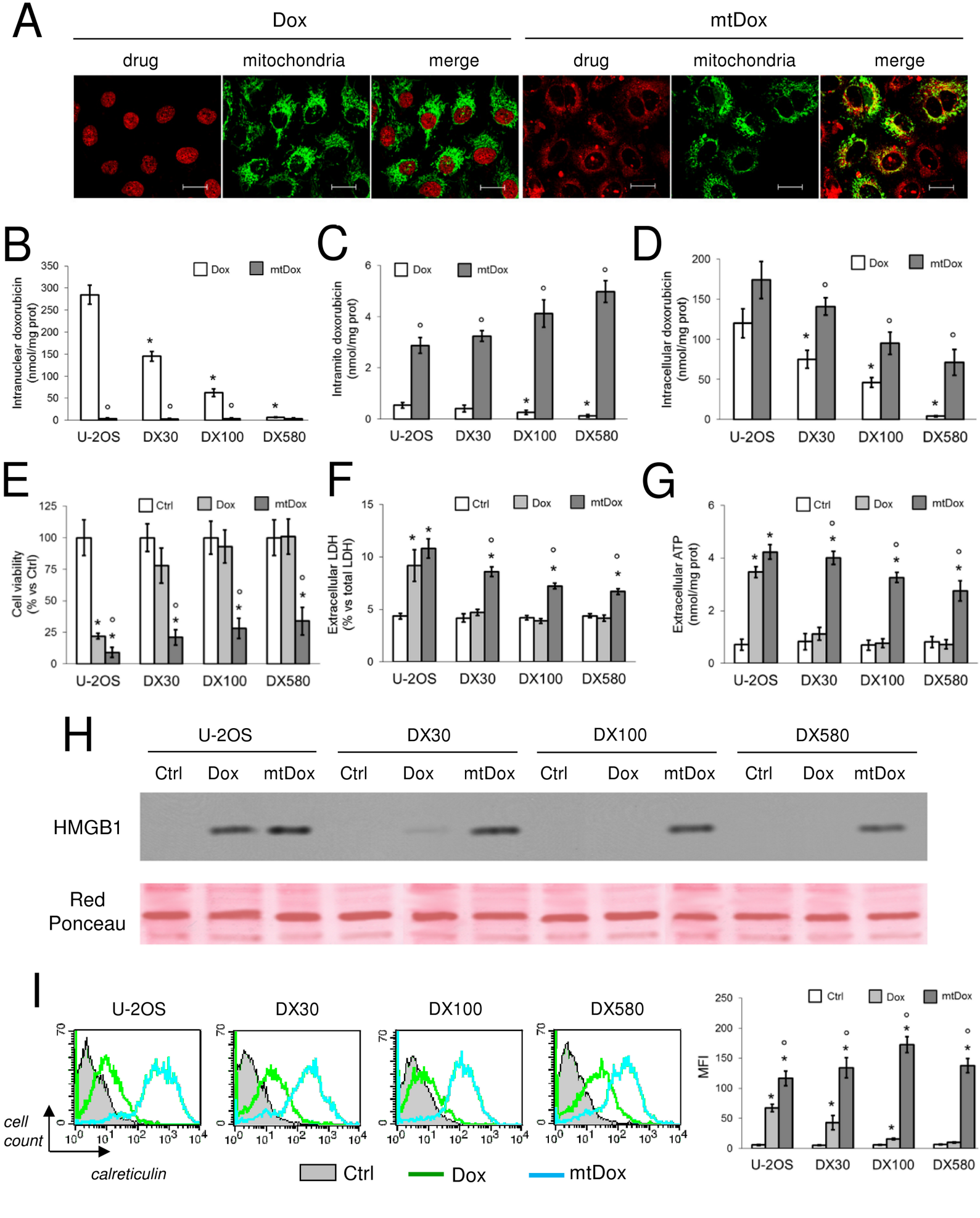
A
Dox
mtDox
drug
mitochondria
merge
drug
mitochondria
merge
B
Intranuclear doxorubicin (nmol/mg prot)
Dox
mtDox
U-2OS
DX30
DX100
DX580
C
Intramito doxorubicin (nmol/mg prot)
Dox
mtDox
U-2OS
DX30
DX100
DX580
D
Intracellular doxorubicin (nmol/mg prot)
Dox
mtDox
U-2OS
DX30
DX100
DX580
E
Cell viability (% vs Ctrl)
Ctrl
Dox
mtDox
U-2OS
DX30
DX100
DX580
F
Extracellular LDH (% vs total LDH)
Ctrl
Dox
mtDox
U-2OS
DX30
DX100
DX580
G
Extracellular ATP (nmol/mg prot)
Ctrl
Dox
mtDox
U-2OS
DX30
DX100
DX580
H
U-2OS
DX30
DX100
DX580
Ctrl
Dox
mtDox
HMGB1
Red Ponceau
I
U-2OS
DX30
DX100
DX580
cell count
calreticulin
Ctrl
Dox
mtDox
MFI
Ctrl
Dox
mtDox
U-2OS
DX30
DX100
DX580

Figure 2

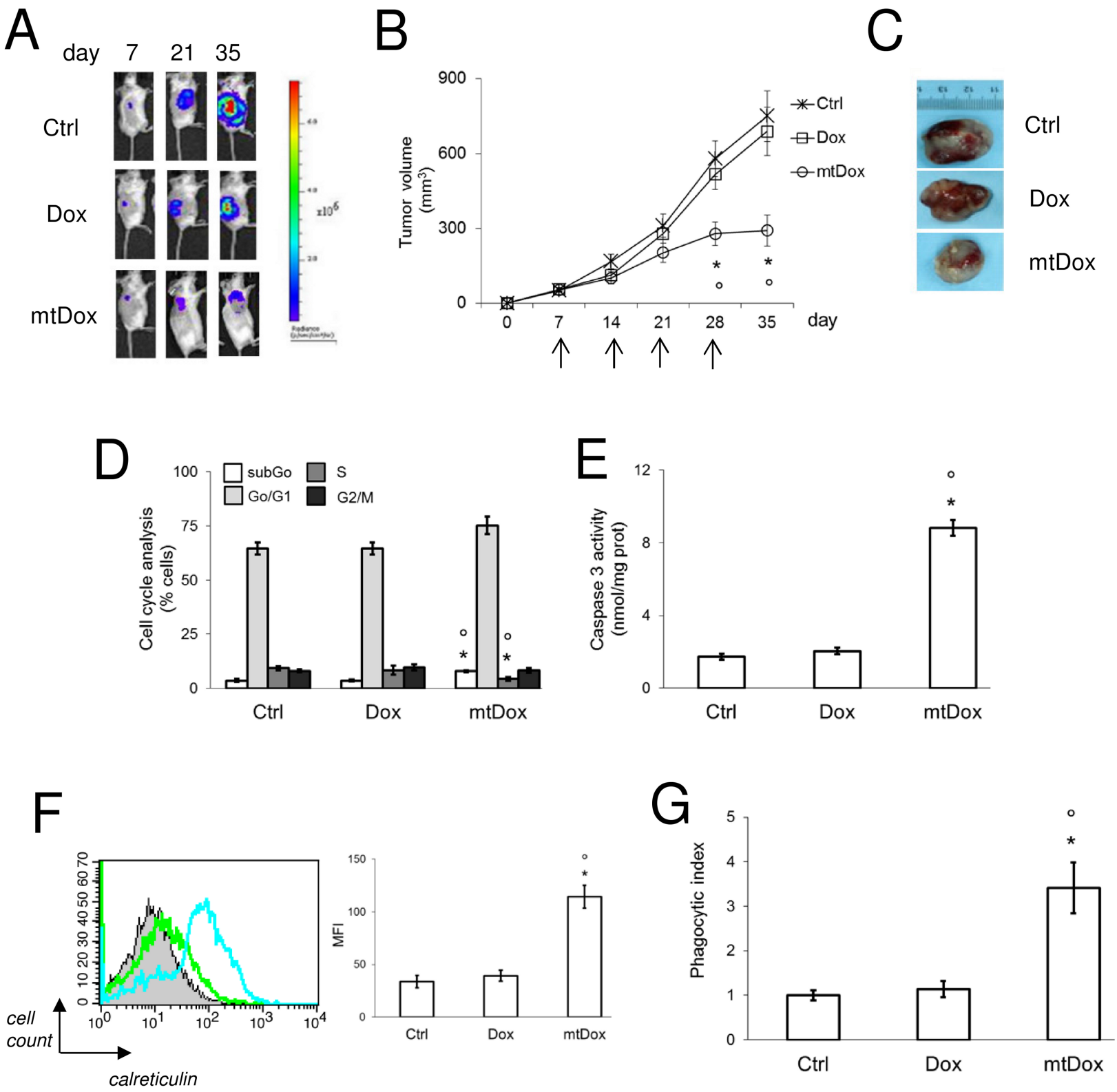
A
day 7 21 35
Ctrl
Dox
mtDox
B
Tumor volume (mm3)
900
600
300
0
0 7 14 21 28 35 day
Ctrl
Dox
mtDox
C
Ctrl
Dox
mtDox
D
subGo
S
Go/G1
G2/M
Cell cycle analysis (% cells)
100
75
50
25
0
Ctrl Dox mtDox
E
Caspase 3 activity (nmol/mg prot)
12
8
4
0
Ctrl Dox mtDox
F
cell count
calreticulin
MFI
150
100
50
0
Ctrl Dox mtDox
G
Phagocytic index
5
4
3
2
1
0
Ctrl Dox mtDox

Figure 3

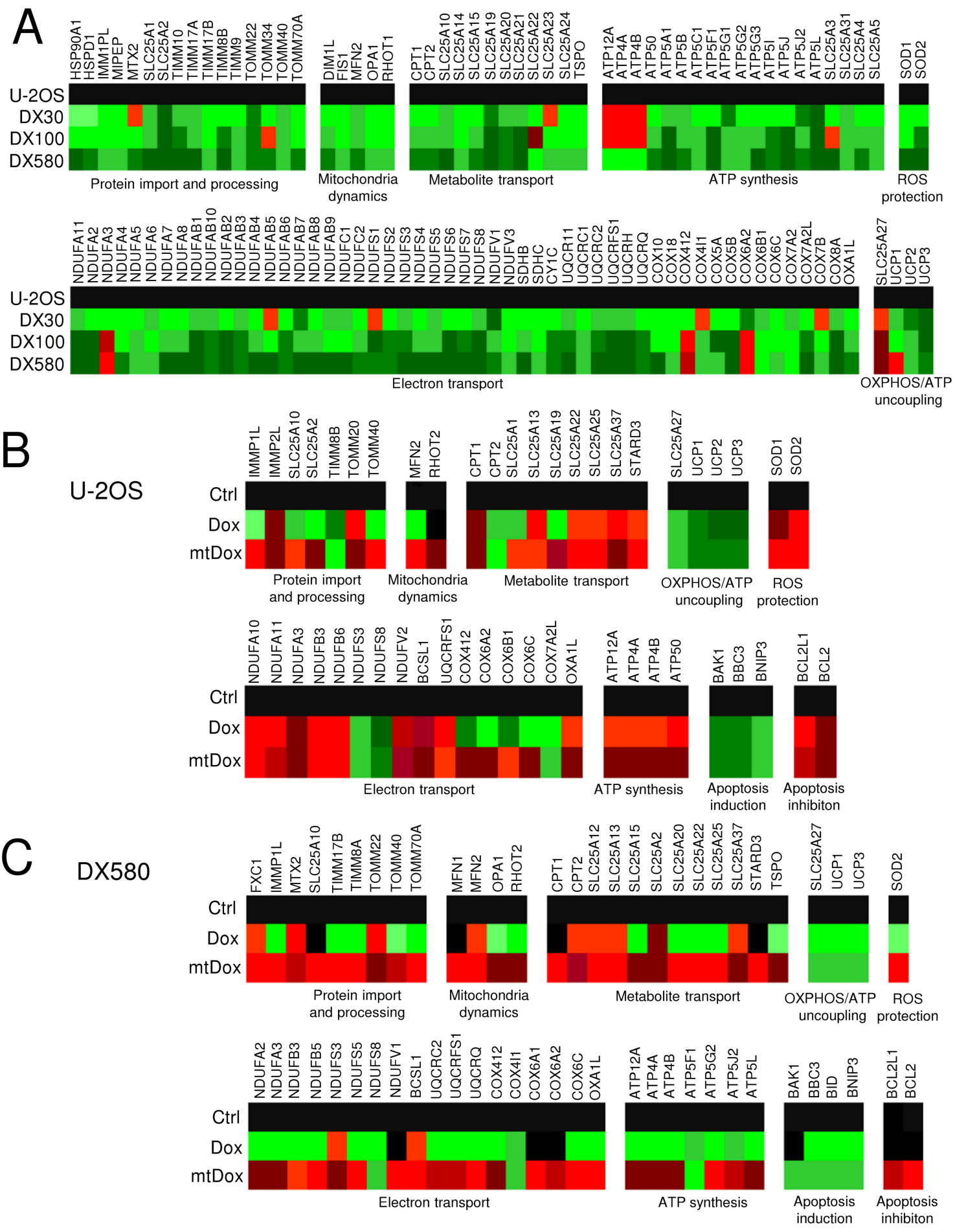
A
HSP90A1
HSPD1
IMM1PL
MIPEP
MTX2
SLC25A1
SLC25A2
TIMM10
TIMM17A
TIMM17B
TIMM8B
TIMM9
TOMM22
TOMM34
TOMM40
TOMM70A
DIM1L
FIS1
MFN2
OPA1
RHOT1
CPT1
CPT2
SLC25A10
SLC25A14
SLC25A15
SLC25A19
SLC25A20
SLC25A21
SLC25A22
SLC25A23
SLC25A24
TSPO
ATP12A
ATP4A
ATP4B
ATP50
ATP5A1
ATP5B
ATP5C1
ATP5F1
ATP5G1
ATP5G2
ATP5G3
ATP5I
ATP5J
ATP5J2
ATP5L
SLC25A3
SLC25A31
SLC25A4
SLC25A5
SOD1
SOD2
U-2OS
DX30
DX100
DX580
Protein import and processing
Mitochondria dynamics
Metabolite transport
ATP synthesis
ROS protection
NDUFA11
NDUFA2
NDUFA3
NDUFA4
NDUFA5
NDUFA6
NDUFA7
NDUFA8
NDUFAB1
NDUFAB10
NDUFAB2
NDUFAB3
NDUFAB4
NDUFAB5
NDUFAB6
NDUFAB7
NDUFAB8
NDUFAB9
NDUFC1
NDUFC2
NDUFS1
NDUFS2
NDUFS3
NDUFS4
NDUFS5
NDUFS6
NDUFS7
NDUFS8
NDUFV1
NDUFV3
SDHB
SDHC
CY1C
UQCR11
UQCRC1
UQCRC2
UQCRFS1
UQCRH
UQCRQ
COX10
COX18
COX412
COX4I1
COX5A
COX5B
COX6A2
COX6B1
COX6C
COX7A2
COX7A2L
COX7B
COX8A
OXA1L
SLC25A27
UCP1
UCP2
UCP3
U-2OS
DX30
DX100
DX580
Electron transport
OXPHOS/ATP uncoupling
B
U-2OS
IMMP1L
IMMP2L
SLC25A10
SLC25A2
TIMM8B
TOMM20
TOMM40
MFN2
RHOT2
CPT1
CPT2
SLC25A1
SLC25A13
SLC25A19
SLC25A22
SLC25A25
SLC25A37
STARD3
SLC25A27
UCP1
UCP2
UCP3
SOD1
SOD2
Ctrl
Dox
mtDox
Protein import and processing
Mitochondria dynamics
Metabolite transport
OXPHOS/ATP uncoupling
ROS protection
NDUFA10
NDUFA11
NDUFA3
NDUFB3
NDUFB6
NDUFS3
NDUFS8
NDUFV2
BCSL1
UQCRFS1
COX412
COX6A2
COX6B1
COX6C
COX7A2L
OXA1L
ATP12A
ATP4A
ATP4B
ATP50
BAK1
BBC3
BNIP3
BCL2L1
BCL2
Ctrl
Dox
mtDox
Electron transport
ATP synthesis
Apoptosis induction
Apoptosis inhibiton
C
DX580
FXC1
IMMP1L
MTX2
SLC25A10
TIMM17B
TIMM8A
TOMM22
TOMM40
TOMM70A
MFN1
MFN2
OPA1
RHOT2
CPT1
CPT2
SLC25A12
SLC25A13
SLC25A15
SLC25A2
SLC25A20
SLC25A22
SLC25A25
SLC25A37
STARD3
TSPO
SLC25A27
UCP1
UCP3
SOD2
Ctrl
Dox
mtDox
Protein import and processing
Mitochondria dynamics
Metabolite transport
OXPHOS/ATP uncoupling
ROS protection
NDUFA2
NDUFA3
NDUFB3
NDUFB5
NDUFS3
NDUFS5
NDUFS8
NDUFV1
BCSL1
UQCRC2
UQCRFS1
UQCRQ
COX412
COX4I1
COX6A1
COX6A2
COX6C
OXA1L
ATP12A
ATP4A
ATP4B
ATP5F1
ATP5G2
ATP5J2
ATP5L
BAK1
BBC3
BID
BNIP3
BCL2L1
BCL2
Ctrl
Dox
mtDox
Electron transport
ATP synthesis
Apoptosis induction
Apoptosis inhibiton
Fold change
<-4
-4
-3
-2
-1
0
1
2
3
4
>4

Figure 4

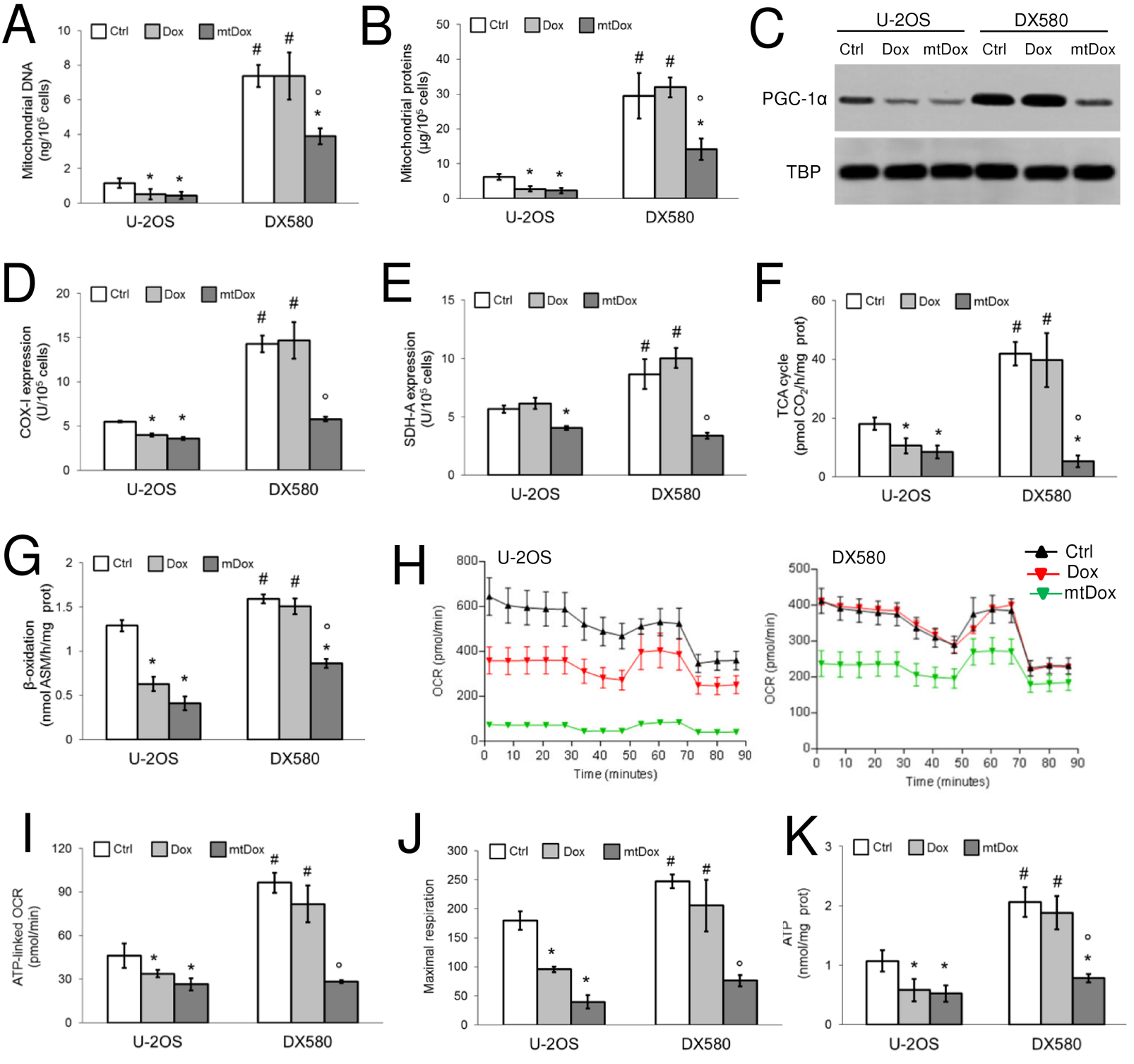
A
Ctrl
Dox
mtDox
Mitochondrial DNA (ng/10⁵ cells)
U-2OS
DX580
B
Mitochondrial proteins (µg/10⁵ cells)
C
U-2OS
DX580
Ctrl
Dox
mtDox
PGC-1α
TBP
D
COX-I expression (U/10⁵ cells)
E
SDH-A expression (U/10⁵ cells)
F
TCA cycle (pmol CO2/h/mg prot)
G
β-oxidation (nmol ASM/h/mg prot)
H
OCR (pmol/min)
Time (minutes)
I
ATP-linked OCR (pmol/min)
J
Maximal respiration
K
ATP (nmol/mg prot)

Figure 5

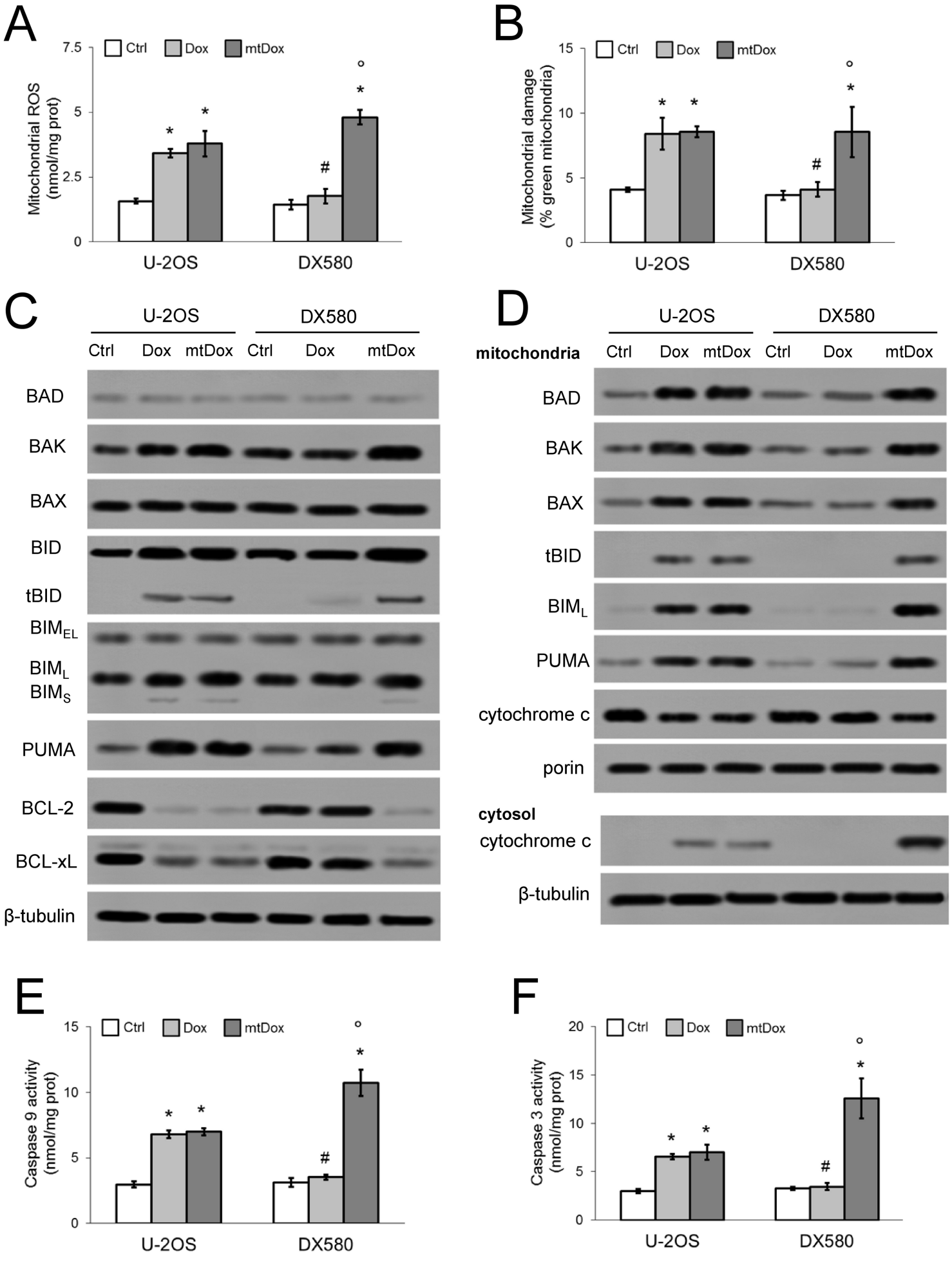
A
Ctrl
Dox
mtDox
Mitochondrial ROS (nmol/mg prot)
7.5
5
2.5
0
U-2OS
DX580
B
Mitochondrial damage (% green mitochondria)
15
10
5
0
C
U-2OS
DX580
Ctrl
Dox
mtDox
BAD
BAK
BAX
BID
tBID
BIM$_{EL}$
BIM$_L$
BIM$_S$
PUMA
BCL-2
BCL-xL
β-tubulin
D
mitochondria
tBID
BIM$_L$
PUMA
cytochrome c
porin
cytosol
cytochrome c
β-tubulin
E
Caspase 9 activity (nmol/mg prot)
F
Caspase 3 activity (nmol/mg prot)
20

Targeting mitochondria to overcome drug resistance in osteosarcoma

Supplementary materials

Supplementary Figures

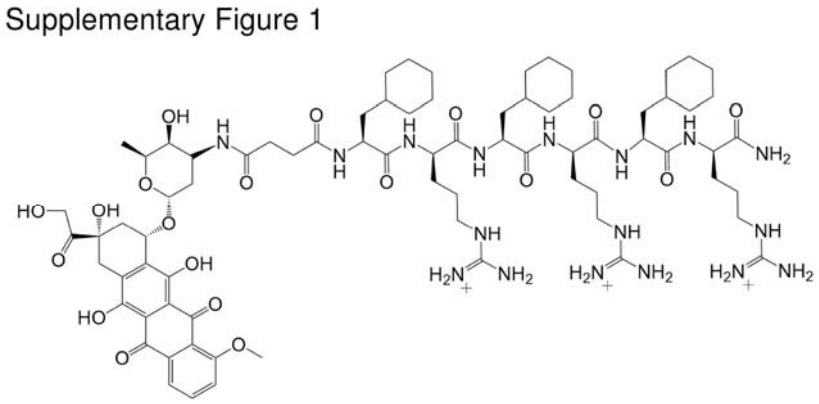

Supplementary Figure S1. Chemical structure of mitochondria-targeted doxorubicin.

Supplementary Figure 2

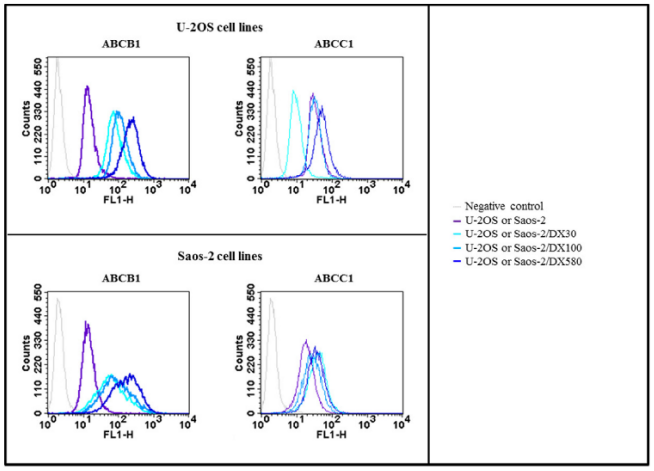

Supplementary Figure S2. Expression of Pgp and MRP1 in doxorubicin-sensitive and doxorubicin-resistant osteosarcoma cells

Human Dox-sensitive U-2OS cells and Dox-resistant variants (U-2OS/DX30, U-2OS/DX100, U-2OS/DX580), human Dox-sensitive Saos-2 cells and Dox-resistant variants (Saos-2/DX30, Saos-2/DX100, Saos-2/DX580) were analyzed for the surface expression of ABCB1/Pgp and ABCC1/MRP1 by flow cytometry in duplicate. The figure is representative of 1 out of 3 experiments.

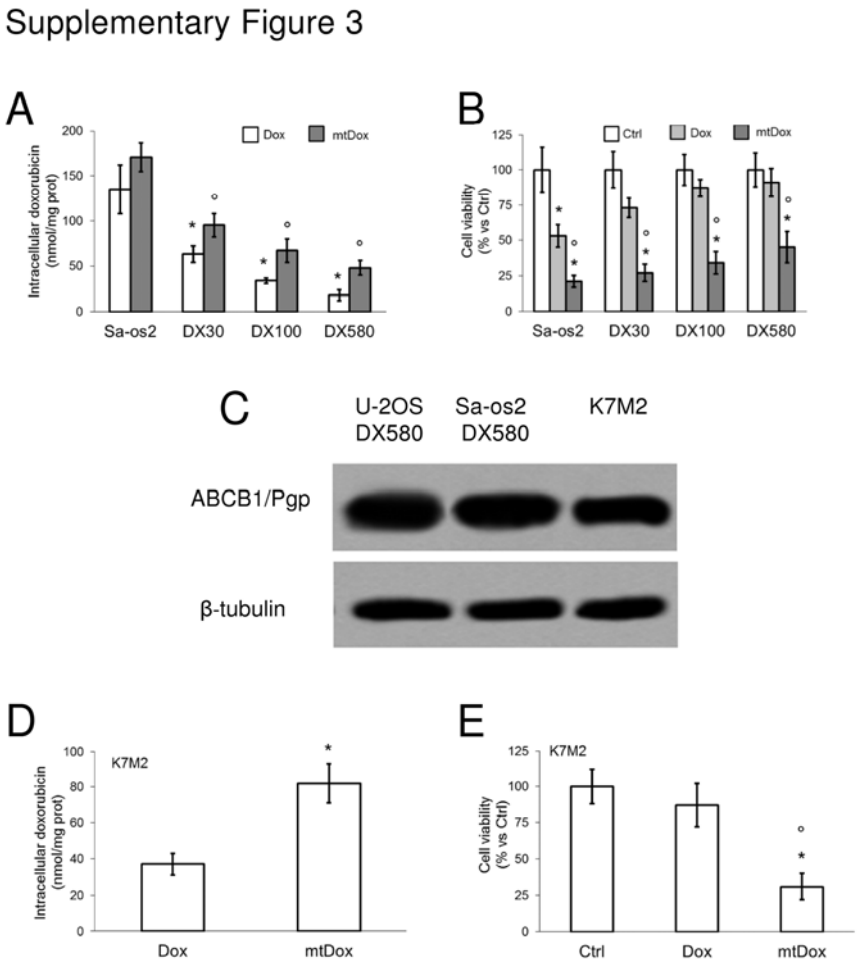

Supplementary Figure S3. Intracellular accumulation and cytotoxicity of mitochondria-targeted doxorubicin in drug-sensitive Saos-2 cells and in their resistant variants, and in K7M2 cells

A. Dox-sensitive Saos-2 cells and Dox-resistant variants (Saos-2/DX30, Saos-2/DX100, Saos-2/DX580) were incubated with 5 μmol/L Dox or mtDox for 24 h. The amount of Dox in whole cell lysates was measured spectrofluorimetrically in duplicate. Data are presented as means ± SD (n= 3). Versus Saos-2 cells: * $p < 0.01$; mtDox versus Dox: ° $p < 0.05$. **B.** Cells were grown for 72 h in fresh medium (Ctrl), in medium containing 5 μmol/L Dox or mtDox, then stained with neutral red solution in quadruplicate. The results were expressed as a percentage of viable cells versus untreated cells. Data are presented as means ± SD (n= 3). Versus respective Ctrl: * $p < 0.005$; mtDox versus Dox: ° $p < 0.005$. C**.** Murine osteosarcoma K7M2 cells were lysed and subjected to the Western blot analysis of ABCB1/Pgp. The resistant U-2OS/DX580 and Saos-2/DX580 variants

were included as control of Pgp-overexpressing cells. The β-tubulin expression was used as a control of equal protein loading. The figure is representative of 1 out of 2 experiments. **D.** K7M2 cells were incubated for 24 h with 5 μmol/L Dox or mtDox. The amount of Dox was measured spectrofluorimetrically in duplicate. Data are presented as means ± SD (n= 3). mtDox versus Dox: * $p < 0.01$. **E**. Cells were grown for 72 h in fresh medium (Ctrl), in medium containing 5 μmol/L Dox or mtDox, then stained with neutral red solution in quadruplicate. The results were expressed as a percentage of viable cells versus untreated cells. Data are presented as means ± SD (n= 3). Versus Ctrl: * $p < 0.002$; mtDox versus Dox: ° $p < 0.002$.

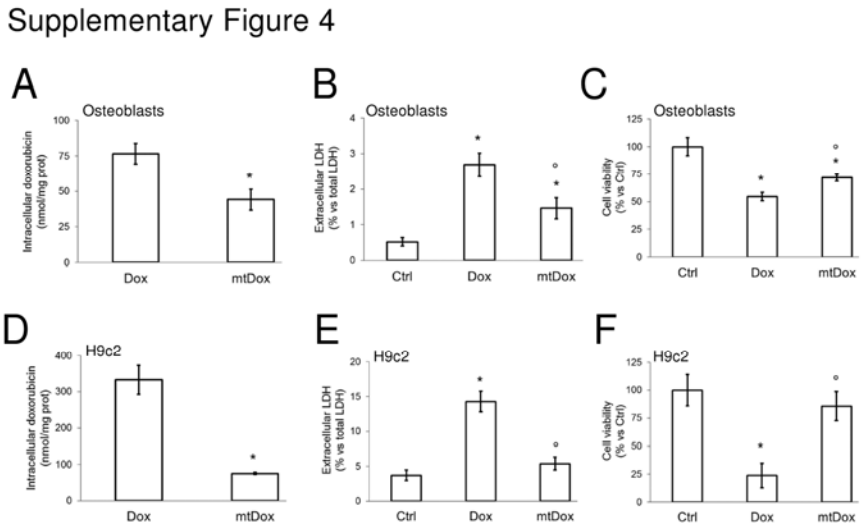

Supplementary Figure S4. Intracellular accumulation and cytotoxicity of mitochondria-targeted doxorubicin in non-transformed osteoblasts and cardiomyocytes

Human non-transformed osteoblasts and rat neonatal H9c2 cardiomyocytes were cultured for 24 h (panels **A, B, D, E**) or 72 h (panels **C**, **F**) in fresh medium (Ctrl), in medium containing 5 μmol/L Dox or mtDox. **A** and **D.** The amount of Dox in whole cell lysates was measured spectrofluorimetrically in duplicate. Data are presented as means $\pm$ SD (n= 3). mtDox versus Dox: * $p < 0.02$. **B** and **E.** The release of LDH in the extracellular medium was measured spectrophotometrically in duplicate. Data are presented as means $\pm$ SD (n= 3). Versus respective Ctrl: * $p < 0.005$; mtDox versus Dox: ° $p < 0.01$. **C** and **F.** Cells were stained with neutral red solution in quadruplicate. The results were expressed as a percentage of viable cells versus untreated cells. Data are presented as means $\pm$ SD (n= 4). Versus respective Ctrl: * $p < 0.01$; mtDox versus Dox: ° $p < 0.02$.

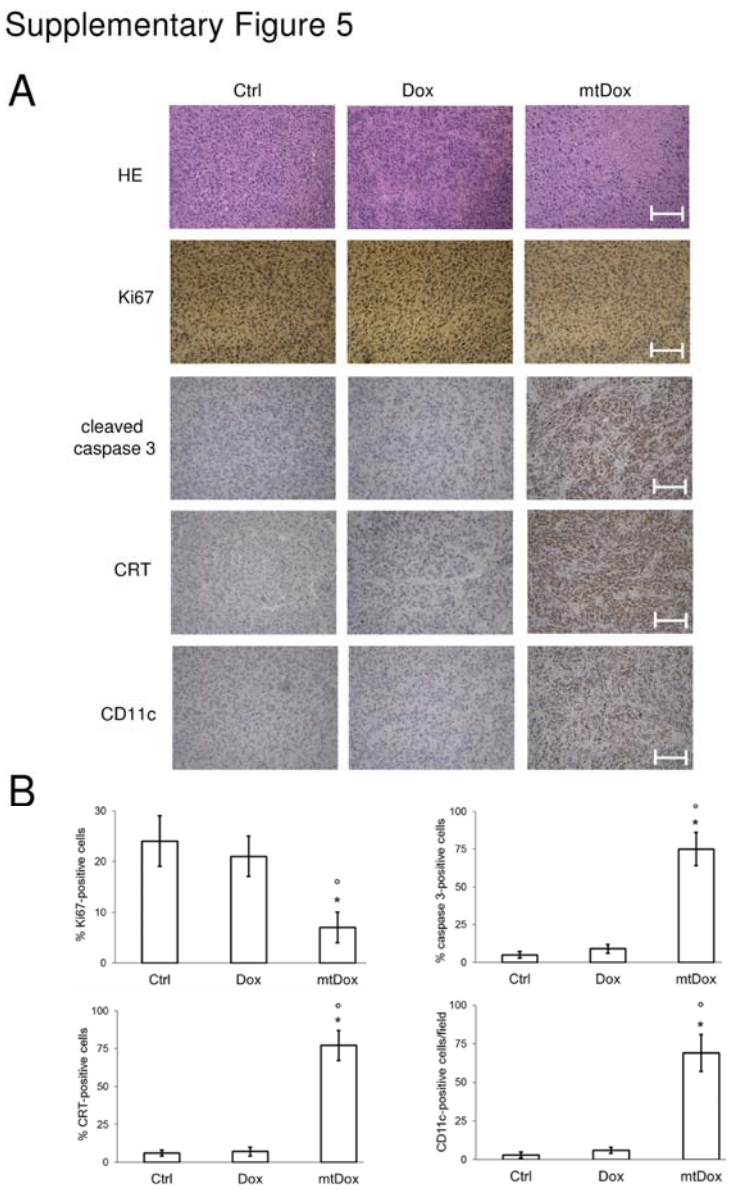

Supplementary Figure S5. Immunohistochemical analysis of drug-resistant osteosarcoma treated with mitochondria-targeted doxorubicin

Six week-old female NOD SCID BALB/c mice were inoculated s.c. with 1 x 10^7 U-2OS cells. When the tumor reached the volume of 50 mm^3 (day 7), the animals were randomized and treated on days 7, 14, 21, 28 as follows: 1) Ctrl group, treated with 0.1 mL saline solution i.v.; 2) Dox group, treated with 5 mg/kg Dox i.v.; 3) mtDox group, treated with 5 mg/kg mitochondria-targeted Dox i.v. Animals were sacrificed on day 35. **A.** Sections of tumors from each group of animals were stained with hematoxylin and eosin (HE) or immunostained for the proliferation marker Ki67, the apoptotic marker cleaved caspase 3, the immunogenic death marker calreticulin (CRT), the DC

marker CD11c. Nuclei were counterstained with hematoxylin. Bar = 10 μm. The photographs are representative of sections from 5 tumors/group. **B. Q**uantification of immunohistochemical images, performed on sections from 5 animals of each group (105-83 nuclei/field). The percentage of proliferating cells was determined by the ratio Ki67-positive nuclei/total number (hematoxylin-positive) of nuclei using ImageJ software (http://imagej.nih.gov/ij/). The ctrl group percentage was considered 100%. The percentage of caspase 3-positive and CRT-positive cells was determined by Photoshop program. The number of CD11c-positive cells/field was calculated by ImageJ software. Data are presented as means ± SD. Versus Ctrl group: * $p < 0.02$; mtDox group versus Dox group: ° $p < 0.01$.

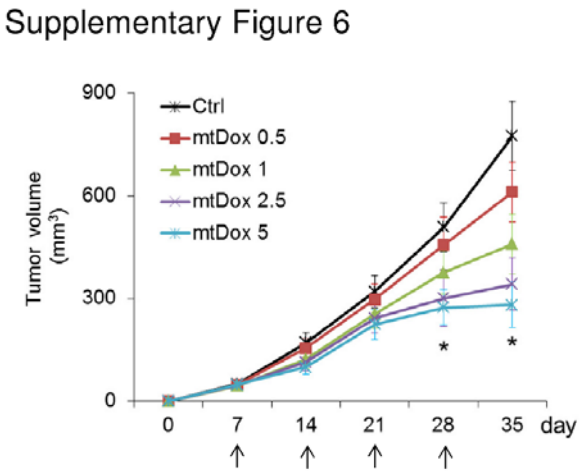

Supplementary Figure S6. Dose-response effects of mitochondria-targeted doxorubicin on drug-resistant osteosarcoma *in vivo*

Six week-old female BALB/c mice were inoculated s.c. with 1 x 10^6 K7M2 cells. When the tumor reached the volume of 50 mm^3 (day 7), the animals (10 mice/group) were randomized and treated on days 7, 14, 21, 28 with 0.1 mL saline solution i.v. (Ctrl group) or with 0.5, 1, 2.5, 5 mg/kg mtDox. Tumor growth monitored by caliper measurements. Arrows represent saline or mtDox injections. Data are presented as means ± SD. 1, 2.5, 5 mg/kg mtDox group versus Ctrl group: * $p < 0.01$.

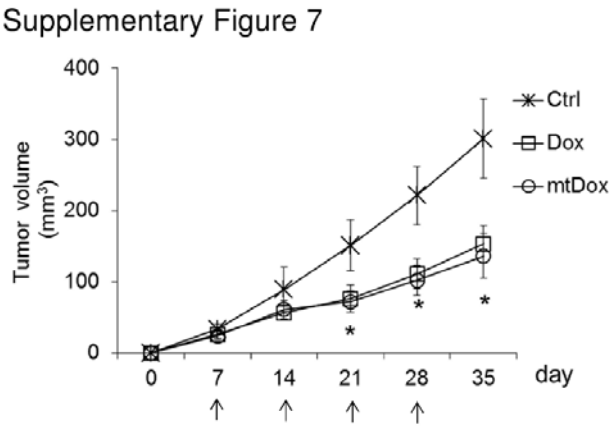

Supplementary Figure S7. Effects of mitochondria-targeted doxorubicin on drug-sensitive osteosarcoma *in vivo*

Six week-old female NOD SCID BALB/c mice were inoculated s.c. with 1 x 10^7 U-2OS cells. When the tumor reached the volume of 50 mm^3 (day 7), the animals were randomized and treated on days 7, 14, 21, 28 as it follows: 1) Ctrl group, treated with 0.1 mL saline solution i.v.; 2) Dox group, treated with 5 mg/kg Dox i.v.; 3) mtDox group, treated with 5 mg/kg mitochondria-targeted Dox i.v. Arrows represent saline or drug injections. Data are presented as means ± SD. Dox/mtDox group versus Ctrl group: * $p < 0.001$.

Supplementary Tables

Supplementary Table S1. IC_{50} (µmol/L) of doxorubicin and mitochondria-targeted doxorubicin

Cell line	Dox	mtDox
U-2OS	3.91 ± 0.43	1.09 ± 0.12 °
U-2OS/DX30	25.62 ± 1.16 *	2.35 ± 0.28 °
U-2OS/DX100	79.67 ± 6.17 *	4.68 ± 0.99 °
U-2OS/DX580	124.18 ± 11.07 *	10.71 ± 0.87 °
Saos-2	4.55 ± 0.71	2.31 ± 0.23 °
Saos-2/DX30	18.78 ± 2.37 *	3.81 ± 0.42 °
Saos-2/DX100	53.29 ± 8.93 *	6.17 ± 0.52 °
Saos-2/DX580	109.82 ± 21.09 *	9.71 ± 0.87 °
K7M2	75.71 ± 4.77	8.54 ± 0.41 °
Primary osteoblasts	4.93 ± 0.29	27.52 ± 4.11 °
H9c2	0.72 ± 0.08	12.39 ± 5.27 °

Cells were incubated for 72 h with increasing concentrations (1 nmol/L-1 mmol/L) of Dox or mtDox, then stained in quadruplicate with neutral red. Data are presented as means ± SD (n = 3). Dox-resistant variants versus their parental cells: * $p < 0.001$; mtDox versus Dox: °$p < 0.001$.

Supplementary Table S2. Expression of mitochondria-related genes in U-2OS cells and resistant variants

Gene	Fold change DX30 versus U-2OS	p value	Fold change DX100 versus U-2OS	p value	Fold change DX580 versus U-2OS	p value	Biological function
AIFM2	1.66	0.02	1.42	0.005	1.04	Ns	Apoptosis induction
ATP12A	**0.34**	0.005	**0.45**	0.02	1.70	Ns	H^+/ATP exchange
ATP4A	**0.33**	0.005	**0.45**	0.02	1.70	Ns	H^+/ATP exchange
ATP4B	**0.34**	0.005	**0.45**	0.02	1.67	Ns	H^+/ATP exchange
ATP50	1.29	Ns	**2.40**	0.001	**3.71**	0.001	ATP synthase subunit
ATP5A1	**2.24**	0.002	**5.82**	0.001	**6.38**	0.001	ATP synthase subunit
ATP5B	**2.09**	0.005	**2.96**	0.001	**3.93**	0.001	ATP synthase subunit
ATP5C1	1.38	0.05	**2.91**	0.001	**2.26**	0.001	ATP synthase subunit
ATP5F1	1.70	0.01	**4.62**	0.001	**4.91**	0.001	ATP synthase subunit
ATP5G1	**3.40**	0.001	**2.53**	0.001	**2.42**	0.001	ATP synthase subunit
ATP5G2	1.72	0.01	**2.24**	0.001	**2.42**	0.001	ATP synthase subunit
ATP5G3	1.80	0.01	**2.29**	0.001	**5.41**	0.001	ATP synthase subunit
ATP5I	1.82	0.005	**3.4**	0.001	**3.93**	0.001	ATP synthase subunit
ATP5J	1.59	0.001	**5.92**	0.001	**6.38**	0.001	ATP synthase subunit
ATP5J2	**3.17**	0.001	**2.06**	0.001	**3.93**	0.001	ATP synthase subunit
ATP5L	**4.41**	0.001	**4.49**	0.001	**10.38**	0.001	ATP synthase subunit
BAK1	1.55	0.02	1.10	Ns	1.42	Ns	Apoptosis induction
BBC3	1.44	Ns	1.52	Ns	0.88	Ns	Apoptosis induction
BCL2	1.35	0.05	0.88	Ns	1.13	Ns	Apoptosis inhibition
BCL2L1	1.78	0.001	0.73	Ns	1.17	Ns	Apoptosis induction
BCS1L	1.82	0.005	1.82	0.001	1.39	0.01	Ubiquinol-cytochrome c reductase assembly
BID	1.55	0.02	1.19	Ns	1.59	Ns	Apoptosis induction
BNIP3	1.18	Ns	1.99	Ns	1.90	Ns	Apoptosis induction
COX10	1.66	0.01	1.41	Ns	**4.02**	0.05	Cytochrome c oxidase assembly
COX18	1.78	0.02	1.40	Ns	**2.05**	0.02	Cytochrome c oxidase assembly
COX412	1.70	Ns	**0.45**	0.02	**0.34**	0.01	Cytochrome c oxidase subunit
COX4I1	0.79	Ns	**2.40**	0.001	**2.39**	0.01	Cytochrome c oxidase assembly
COX5A	1.95	0.005	**4.16**	0.001	**2.59**	0.001	Cytochrome c oxidase subunit
COX5B	1.95	0.005	**4.16**	0.001	**5.81**	0.001	Cytochrome c oxidase subunit
COX6A1	1.70	0.01	0.81	0.001	0.71	0.02	Cytochrome c oxidase subunit
COX6A2	**3.32**	0.01	**0.41**	0.001	**0.34**	0.001	Cytochrome c oxidase subunit
COX6B1	**2.41**	0.005	1.16	0.001	1.71	0.001	Cytochrome c oxidase assembly/regulation
COX6C	1.38	0.05	1.49	0.05	**2.26**	0.001	Cytochrome c oxidase assembly/regulation
COX7A2	**2.24**	0.005	1.86	0.001	1.71	0.001	Cytochrome c oxidase assembly/regulation
COX7A2L	1.29	Ns	**3.81**	0.001	**4.21**	0.001	Cytochrome c oxidase assembly/regulation
COX7B	0.85	0.002	1.96	0.001	**2.11**	0.001	Cytochrome c oxidase subunit

COX8A	**2.09**	0.001	**4.53**	0.001	**4.51**	0.001	Cytochrome c oxidase regulation
CPT1	1.66	0.01	**2.05**	0.05	**3.30**	0.05	Long chain fatty acylcoA import/β-oxidation
CPT2	1.55	0.02	**2.04**	0.05	**3.42**	0.01	Long chain fatty acylcoA import/β-oxidation
CYC1	1.95	0.005	**3.24**	0.001	**3.98**	0.001	Electron transport
DMM1L	1.91	0.01	**2.16**	0.02	**3.18**	0.05	Control of mitochondria morphology
FIS1	1.35	0.05	1.52	Ns	**2.71**	0.05	Control of mitochondria fission
FXC1	1.45	0.05	0.78	Ns	1.05	Ns	Mitochondrial proteins import
HSP90A1	1.26	Ns	**2.26**	0.05	**4.40**	0.05	Proteins chaperon
HSPD1	1.26	Ns	**2.16**	0.05	**3.33**	0.05	Mitochondrial proteins chaperon
IMMP1L	1.45	0.05	1.24	0.05	**2.01**	0.05	Mitochondrial proteins processing/import
IMMP2L	0.59	0.001	0.80	Ns	1.56	Ns	Mitochondrial proteins processing/import
LRPPRC	1.10	Ns	1.42	Ns	1.59	Ns	Mitochondrial transcription factor
MFN1	0.63	0.02	0.86	Ns	1.15	Ns	Control of mitochondria fusion
MFN2	**2.19**	0.002	**2.43**	0.05	**3.49**	0.05	Control of mitochondria fusion
MIPEP	1.78	0.01	1.39	Ns	**2.47**	0.05	Mitochondrial proteins processing
MPV17	1.66	0.01	1.18	Ns	1.45	0.005	Metabolism of mitochondrial ROS
MTX2	0.72	0.05	1.18	Ns	**3.11**	0.001	Mitochondrial proteins import
NDUFA1	1.82	0.005	1.40	0.001	1.71	0.001	NADH:ubiquinone oxidoreductase subunit
NDUFA10	1.70	0.01	1.38	0.001	1.70	0.002	NADH:ubiquinone oxidoreductase subunit
NDUFA11	**2.58**	0.001	**5.29**	0.001	**6.84**	0.001	NADH:ubiquinone oxidoreductase subunit
NDUFA2	1.70	0.01	**5.16**	0.001	**6.41**	0.001	NADH:ubiquinone oxidoreductase assembly
NDUFA3	1.95	0.005	**0.29**	0.001	**0.40**	0.05	NADH:ubiquinone oxidoreductase subunit
NDUFA4	1.82	0.005	1.91	0.001	**3.96**	0.001	NADH:ubiquinone oxidoreductase subunit
NDUFA5	1.70	0.01	**2.19**	0.001	**2.26**	0.001	NADH:ubiquinone oxidoreductase subunit
NDUFA6	**2.09**	0.005	1.91	0.001	**2.11**	0.001	NADH:ubiquinone oxidoreductase subunit
NDUFA7	1.48	0.02	**2.24**	0.001	**4.21**	0.001	NADH:ubiquinone oxidoreductase subunit
NDUFA8	1.70	0.01	**2.78**	0.001	**8.38**	0.001	NADH:ubiquinone oxidoreductase subunit
NDUFAB1	**2.76**	0.001	**4.12**	0.001	**6.35**	0.001	NADH:ubiquinone oxidoreductase subunit
NDUFAB10	**2.76**	0.001	**3.91**	0.001	**3.93**	0.001	NADH:ubiquinone oxidoreductase subunit
NDUFB2	1.95	0.005	**5.92**	0.001	**6.38**	0.001	NADH:ubiquinone oxidoreductase subunit
NDUFB3	**2.09**	0.005	**3.81**	0.001	**3.97**	0.001	NADH:ubiquinone oxidoreductase subunit
NDUFB4	1.82	0.005	**2.59**	0.001	**5.16**	0.001	NADH:ubiquinone oxidoreductase subunit
NDUFB5	0.79	Ns	1.71	0.001	**4.19**	0.001	NADH:ubiquinone oxidoreductase subunit
NDUFB6	1.59	0.01	**3.67**	0.001	**3.91**	0.001	NADH:ubiquinone oxidoreductase subunit
NDUFB7	**3.65**	0.005	**2.24**	0.001	**7.86**	0.001	NADH:ubiquinone oxidoreductase subunit
NDUFB8	1.82	0.005	**2.42**	0.001	**8.38**	0.001	NADH:ubiquinone oxidoreductase subunit
NDUFB9	**2.96**	0.001	1.83	0.001	**6.35**	0.001	NADH:ubiquinone oxidoreductase subunit
NDUFC1	**2.24**	0.002	1.26	0.001	**4.19**	0.001	NADH:ubiquinone oxidoreductase subunit
NDUFC2	1.38	0.05	**2.26**	0.001	**3.40**	0.001	NADH:ubiquinone oxidoreductase subunit
NDUFS1	0.85	Ns	**4.81**	0.001	**3.67**	0.001	NADH:ubiquinone oxidoreductase subunit
NDUFS2	1.29	Ns	**3.65**	0.001	**3.19**	0.001	NADH:ubiquinone oxidoreductase subunit
NDUFS3	**2.41**	0.002	**3.19**	0.001	**5.53**	0.001	NADH:ubiquinone oxidoreductase subunit

NDUFS4	1.59	0.01	**2.59**	0.001	**4.49**	0.001	NADH:ubiquinone oxidoreductase subunit
NDUFS5	**2.24**	0.002	**2.78**	0.001	**5.16**	0.001	NADH:ubiquinone oxidoreductase subunit
NDUFS6	**2.24**	0.005	**4.81**	0.001	**4.84**	0.001	NADH:ubiquinone oxidoreductase subunit
NDUFS7	1.82	0.001	**3.93**	0.001	**4.49**	0.001	NADH:ubiquinone oxidoreductase subunit
NDUFS8	**2.76**	0.001	**14.49**	0.001	**16.76**	0.001	NADH:ubiquinone oxidoreductase subunit
NDUFV1	**4.19**	0.001	**2.98**	0.001	**3.65**	0.001	NADH:ubiquinone oxidoreductase subunit
NDUFV2	1.59	0.01	1.29	0.001	1.05	Ns	NADH:ubiquinone oxidoreductase subunit
NDUFV3	1.20	Ns	1.49	0.002	**2.24**	0.001	NADH:ubiquinone oxidoreductase subunit
OPA1	1.45	0.05	1.79	0.05	**2.01**	0.05	Control of mitochondria network
OXA1L	1.59	0.005	**2.11**	0.001	**3.65**	0.001	Cytochrome c oxidase assembly
RHOT1	1.55	0.02	1.39	Ns	**2.71**	0.05	Control of mitochondria fission and fusion
RHOT2	1.91	0.005	0.62	Ns	1.15	Ns	Control of mitochondria fission and fusion
SDHA	1.17	Ns	1.48	0.005	1.83	0.001	Succinate dehydrogenase subunit
SDHB	1.59	0.01	**2.29**	0.001	**4.21**	0.001	Succinate dehydrogenase subunit
SDHC	1.38	0.05	1.58	0.001	1.83	0.001	Succinate dehydrogenase subunit
SDHD	1.29	Ns	1.35	0.001	**2.98**	0.001	Succinate dehydrogenase subunit
SH3SGLB1	1.45	0.05	1.84	Ns	1.53	Ns	Apoptosis induction
SLC25A1	**2.52**	0.002	**2.74**	0.02	**5.29**	0.05	Tricarboxylic acids import
SLC25A10	**2.35**	0.005	**2.66**	0.02	**6.22**	0.05	Mitochondrial proteins import
SLC25A12	1.78	0.01	1.39	0.02	1.96	0.02	Dicarboxylic acids import
SLC25A13	1.02	Ns	1.50	Ns	1.87	Ns	Aspartic acid/glutamic acid exchange
SLC25A14	1.91	0.01	1.42	Ns	**2.30**	0.02	Aspartic acid/glutamic acid exchange
SLC25A15	1.55	0.02	**2.01**	0.05	**3.57**	0.05	Ornithine import
SLC25A19	**3.10**	0.002	**4.01**	0.05	**6.93**	0.05	Thiamine pyrophosphate import
SLC25A2	**4.09**	0.001	**4.53**	0.05	**4.70**	0.05	Mitochondrial proteins import
SLC25A20	**2.46**	0.002	**3.10**	0.05	**3.74**	0.001	Carnitine/acylcarnitine translocation
SLC25A21	**2.76**	0.01	**5.07**	0.05	**5.77**	0.05	Oxodicarboxylic acids import
SLC25A22	1.35	0.05	**0.14**	0.05	1.29	0.05	Glutamate import
SLC25A23	0.72	0.05	1.39	Ns	**2.01**	0.05	Phosphate import
SLC25A24	1.66	0.01	1.71	0.01	**2.77**	0.05	Phosphate import
SLC25A25	1.35	0.05	0.96	0.01	1.07	Ns	Phosphate import
SLC25A27	0.59	0.01	**0.16**	0.01	**0.13**	0.001	OXPHOS/ATP synthesis uncoupling
SLC25A3	1.78	0.01	0.82	Ns	**4.30**	0.05	Phosphate/hydroxyl ions exchange
SLC25A31	**2.44**	0.01	**2.52**	0.05	**2.41**	0.005	Adenine nucleotide translocation
SLC25A37	1.55	0.02	0.92	Ns	0.74	Ns	Iron import
SLC25A4	1.10	Ns	**2.98**	0.05	**3.18**	0.05	Adenine nucleotide translocation
SLC25A5	1.26	Ns	**2.72**	0.05	**2.65**	0.05	Adenine nucleotide translocation
SOD1	1.26	Ns	1.09	Ns	**4.01**	0.05	ROS protection (cytosol)
SOD2	1.48	0.005	**3.39**	0.001	**4.30**	0.001	ROS protection (mitochondria)
STARD3	1.02	Ns	0.94	Ns	1.07	Ns	Cholesterol import
TIMM10	**2.05**	0.005	**3.34**	0.05	**4.30**	0.05	Protein insertion in the inner membrane
TIMM17A	**2.35**	0.005	**2.78**	0.02	**4.72**	0.05	Protein insertion in the inner membrane

TIMM17B	1.10	Ns	1.45	Ns	**2.01**	0.05	Protein insertion in the inner membrane
TIMM8A	1.91	0.01	1.88	Ns	**3.66**	0.05	Protein insertion in the inner membrane
TIMM8B	1.66	0.01	**3.58**	0.02	**5.54**	0.05	Protein insertion in the inner membrane
TIMM9	1.26	Ns	**2.84**	0.05	**2.30**	0.05	Protein insertion in the inner membrane
TOMM20	1.35	0.05	1.46	Ns	1.35	0.05	Mitochondrial proteins import
TOMM22	**3.35**	0.01	**3.13**	0.05	**3.01**	0.05	Mitochondrial proteins import
TOMM34	1.45	0.05	0.90	Ns	**3.66**	0.05	Mitochondrial proteins import
TOMM40	**2.19**	0.005	**2.48**	0.02	**2.65**	0.01	Mitochondrial proteins import
TOMM70A	1.78	0.01	1.75	0.01	**3.74**	0.002	Mitochondrial proteins import
TSPO	1.18	Ns	1.42	Ns	**2.25**	0.05	Cholesterol import
UCP1	**2.44**	0.05	1.34	Ns	**0.42**	0.05	OXPHOS/ATP synthesis uncoupling
UCP2	**3.34**	0.005	**2.12**	0.05	**2.10**	0.05	OXPHOS/ATP synthesis uncoupling
UCP3	**9.19**	0.001	**9.01**	0.05	**3.12**	0.05	OXPHOS/ATP synthesis uncoupling
UQCR11	**2.58**	0.001	**3.42**	0.001	**4.81**	0.001	Ubiquinol-cytochrome c reductase subunit
UQCRC1	1.29	Ns	**2.22**	0.001	**2.96**	0.001	Ubiquinol-cytochrome c reductase subunit
UQCRC2	**2.41**	0.002	**3.67**	0.001	**5.53**	0.001	Ubiquinol-cytochrome c reductase subunit
UQRCFS1	**2.09**	0.002	**8.42**	0.001	**15.63**	0.001	Ubiquinol-cytochrome c reductase subunit
UQCRH	**2.41**	0.002	**5.56**	0.001	**10.31**	0.001	Ubiquinol-cytochrome c reductase subunit
UQCRQ	1.95	0.005	1.71	0.001	**3.40**	0.001	Ubiquinol-cytochrome c reductase subunit

OXPHOS: oxidative phosphorylation.

Fold-Change (2^(- Delta Delta Ct)) is the normalized gene expression (2^(- Delta Ct)) in U-2OS/DX30, U-2OS/DX100 or U-2OS/DX580 cells, divided the normalized gene expression (2^(- Delta Ct)) in U-2OS cells (n= 4), where Ct is the threshold cycle in qRT-PCR; when the fold-change is less than 1, the value is the negative inverse of the fold-change. Ns: not significant. Bold characters: up- or down-regulation more than two-fold.

Supplementary Table S3. Expression of mitochondria-related genes in U-2OS cells untreated and treated with doxorubicin or mitochondria-targeted doxorubicin

Gene	Fold change Dox versus Ctrl	p value	Fold change mtDox versus Ctrl	p value	Biological function
AIFM2	1.83	0.05	0.71	0.02	Apoptosis induction
ATP12A	0.80	0.001	**0.21**	0.001	H^+/ATP exchange
ATP4A	0.71	0.001	**0.22**	0.001	H^+/ATP exchange
ATP4B	0.80	0.001	**0.21**	0.001	H^+/ATP exchange
ATP50	**0.35**	0.001	**0.06**	0.001	ATP synthase subunit
ATP5A1	1.29	0.005	1.99	0.005	ATP synthase subunit
ATP5B	1.21	0.02	1.39	0.002	ATP synthase subunit
ATP5C1	0.86	0.05	1.13	Ns	ATP synthase subunit
ATP5F1	1.39	0.005	1.26	0.01	ATP synthase subunit
ATP5G1	1.30	0.01	1.06	Ns	ATP synthase subunit
ATP5G2	0.65	0.001	1.39	0.02	ATP synthase subunit
ATP5G3	0.99	0.05	1.21	0.05	ATP synthase subunit
ATP5I	0.70	0.002	0.68	0.01	ATP synthase subunit
ATP5J	1.49	0.002	1.11	0.01	ATP synthase subunit
ATP5J2	1.06	Ns	1.97	0.001	ATP synthase subunit
ATP5L	1.84	0.001	1.21	0.02	ATP synthase subunit
BAK1	**3.42**	0.05	**3.72**	0.001	Apoptosis induction
BBC3	**3.46**	0.05	**3.17**	0.001	Apoptosis induction
BCL2	**0.20**	0.05	**0.10**	0.001	Apoptosis inhibition
BCL2L1	**0.48**	0.05	**0.31**	0.005	Apoptosis inhibition
BCS1L	**0.28**	0.001	**0.21**	0.001	Ubiquinol-cytochrome c reductase assembly
BID	1.65	0.05	**2.76**	0.05	Apoptosis induction
BNIP3	**2.48**	0.05	**2.06**	0.05	Apoptosis induction
COX10	1.01	Ns	1	Ns	Cytochrome c oxidase assembly
COX18	0.54	0.05	0.66	0.005	Cytochrome c oxidase assembly
COX412	**3.20**	0.001	**0.21**	0.001	Cytochrome c oxidase subunit
COX4I1	0.92	Ns	1.97	0.001	Cytochrome c oxidase assembly
COX5A	1.30	0.01	0.99	0.005	Cytochrome c oxidase subunit
COX5B	1.06	Ns	1.60	0.001	Cytochrome c oxidase subunit
COX6A1	0.70	0.002	0.57	0.001	Cytochrome c oxidase subunit
COX6A2	1.13	0.005	**0.10**	0.001	Cytochrome c oxidase subunit
COX6B1	**3.20**	0.001	0.92	Ns	Cytochrome c oxidase assembly/regulation
COX6C	1.21	0.02	**0.21**	0.001	Cytochrome c oxidase assembly/regulation
COX7A2	0.75	0.005	1.21	0.02	Cytochrome c oxidase assembly/regulation
COX7A2L	1.81	0.001	**2.26**	0.002	Cytochrome c oxidase assembly/regulation
COX7B	0.80	0.01	1.30	0.01	Cytochrome c oxidase subunit

COX8A	1.71	0.001	1.30	0.01	Cytochrome c oxidase regulation
CPT1	**0.18**	0.001	**0.18**	0.001	Long chain fatty acylcoA import/β-oxidation
CPT2	**2.06**	0.05	0.54	0.005	Long chain fatty acylcoA import/β-oxidation
CYC1	0.98	Ns	1.06	Ns	Electron transport
DMM1L	0.96	Ns	1.06	Ns	Control of mitochondria morphology
FIS1	1.42	0.05	1.24	Ns	Control of mitochondria fission
FXC1	0.56	0.05	0.60	0.05	Mitochondrial proteins import
HSP90A1	0.92	Ns	1.20	Ns	Proteins chaperon
HSPD1	0.58	Ns	1.09	Ns	Mitochondrial proteins chaperon
IMMP1L	0.66	0.05	**0.41**	0.001	Mitochondrial proteins processing/import
IMMP2L	**0.16**	0.001	**0.24**	0.001	Mitochondrial proteins processing/import
LRPPRC	0.58	Ns	0.95	Ns	Mitochondrial transcription factor
MFN1	0.55	0.05	1.09	Ns	Control of mitochondria fusion
MFN2	1.39	0.05	**0.36**	0.001	Control of mitochondria fusion
MIPEP	1.13	Ns	0.79	0.01	Mitochondrial proteins processing
MPV17	1.33	Ns	0.83	0.05	Metabolism of mitochondrial ROS
MTX2	1.63	0.005	1.15	Ns	Mitochondrial proteins import
NDUFA1	0.75	0.005	1.30	0.01	NADH:ubiquinone oxidoreductase subunit
NDUFA10	**0.46**	0.001	**0.35**	0.005	NADH:ubiquinone oxidoreductase subunit
NDUFA11	**0.43**	0.001	**0.27**	0.001	NADH:ubiquinone oxidoreductase subunit
NDUFA2	1.71	0.001	1.91	0.005	NADH:ubiquinone oxidoreductase assembly
NDUFA3	**0.24**	0.001	**0.10**	0.001	NADH:ubiquinone oxidoreductase subunit
NDUFA4	0.70	0.002	1.13	Ns	NADH:ubiquinone oxidoreductase subunit
NDUFA5	0.75	0.005	1.06	Ns	NADH:ubiquinone oxidoreductase subunit
NDUFA6	1.06	Ns	1.30	0.01	NADH:ubiquinone oxidoreductase subunit
NDUFA7	0.86	0.05	1.30	0.01	NADH:ubiquinone oxidoreductase subunit
NDUFA8	1.26	0.002	1.42	0.001	NADH:ubiquinone oxidoreductase subunit
NDUFAB1	1.39	0.005	1.71	0,001	NADH:ubiquinone oxidoreductase subunit
NDUFAB10	0.86	0.05	1.13	Ns	NADH:ubiquinone oxidoreductase subunit
NDUFB2	0.79	0.001	1.46	0.005	NADH:ubiquinone oxidoreductase subunit
NDUFB3	**0.42**	0.001	**0.36**	0.001	NADH:ubiquinone oxidoreductase subunit
NDUFB4	0.98	Ns	1.84	0.005	NADH:ubiquinone oxidoreductase subunit
NDUFB5	1.06	Ns	1.26	0.01	NADH:ubiquinone oxidoreductase subunit
NDUFB6	**0.36**	Ns	**0.37**	0.001	NADH:ubiquinone oxidoreductase subunit
NDUFB7	3.20	0.001	1.97	0.001	NADH:ubiquinone oxidoreductase subunit
NDUFB8	1.13	Ns	1.30	0.005	NADH:ubiquinone oxidoreductase subunit
NDUFB9	1.20	0.05	0.75	0.005	NADH:ubiquinone oxidoreductase subunit
NDUFC1	1.06	Ns	1.49	0.002	NADH:ubiquinone oxidoreductase subunit
NDUFC2	1.30	0.01	1.60	0.001	NADH:ubiquinone oxidoreductase subunit
NDUFS1	0.86	0.05	1.11	Ns	NADH:ubiquinone oxidoreductase subunit
NDUFS2	0.92	Ns	1.60	0.001	NADH:ubiquinone oxidoreductase subunit
NDUFS3	**2.11**	0.001	**2.11**	0.001	NADH:ubiquinone oxidoreductase subunit

NDUFS4	0.70	0.002	0.97	0.001	NADH:ubiquinone oxidoreductase subunit
NDUFS5	1.30	0.01	1.39	0.02	NADH:ubiquinone oxidoreductase subunit
NDUFS6	1.84	0.005	1.84	0.001	NADH:ubiquinone oxidoreductase subunit
NDUFS7	1.60	0.001	1.84	0.001	NADH:ubiquinone oxidoreductase subunit
NDUFS8	**4.22**	0.001	**3.43**	0.001	NADH:ubiquinone oxidoreductase subunit
NDUFV1	0.98	Ns	0.70	0.02	NADH:ubiquinone oxidoreductase subunit
NDUFV2	**0.30**	0.001	**0.25**	0.001	NADH:ubiquinone oxidoreductase subunit
NDUFV3	0.92	Ns	1.49	0.002	NADH:ubiquinone oxidoreductase subunit
OPA1	0.84	Ns	0.60	0.005	Control of mitochondria network
OXA1L	0.80	0.001	**0.21**	0.001	Cytochrome c oxidase assembly
RHOT1	0.56	0.05	1	Ns	Control of mitochondria fission and fusion
RHOT2	1.03	Ns	**0.22**	0.02	Control of mitochondria fission and fusion
SDHA	0.65	0.001	0.94	Ns	Succinate dehydrogenase subunit
SDHB	1.49	0.002	1.65	0.01	Succinate dehydrogenase subunit
SDHC	0.91	Ns	1.71	0.02	Succinate dehydrogenase subunit
SDHD	1.71	0.001	1.42	0.01	Succinate dehydrogenase subunit
SH3SGLB1	1.27	0.005	1.51	Ns	Apoptosis induction
SLC25A1	**2.42**	0.001	0.76	0.005	Tricarboxylic acids import
SLC25A10	**2.98**	0.001	0.69	0.005	Mitochondrial proteins import
SLC25A12	0.59	0.05	0.62	0.005	Dicarboxylic acids import
SLC25A13	**0.41**	0.01	0.52	0.02	Aspartic acid/glutamic acid exchange
SLC25A14	1.15	Ns	0.66	0.05	Aspartic acid/glutamic acid exchange
SLC25A15	1.48	0.05	1.06	Ns	Ornithine import
SLC25A19	1.88	0.05	**0.29**	0.01	Thiamine pyrophosphate import
SLC25A2	1.88	0.02	**0.19**	0.001	Mitochondrial proteins import
SLC25A20	0.98	Ns	0.55	0.01	Carnitine/acylcarnitine translocation
SLC25A21	0.91	Ns	0.76	0.005	Oxodicarboxylic acids import
SLC25A22	0.82	Ns	**0.40**	0.001	Glutamate import
SLC25A23	0.96	Ns	1.26	Ns	Phosphate import
SLC25A24	1.10	Ns	0.91	Ns	Phosphate import
SLC25A25	0.56	0.05	**0.41**	0.02	Phosphate import
SLC25A27	**2.10**	0.001	**2.55**	0.05	OXPHOS/ATP synthesis uncoupling
SLC25A3	1.49	0.05	1.51	Ns	Phosphate/hydroxyl ions exchange
SLC25A31	1.01	Ns	1.09	Ns	Adenine nucleotide translocation
SLC25A37	**0.41**	0.01	**0.19**	0.001	Iron import
SLC25A4	1.60	0.05	1.58	Ns	Adenine nucleotide translocation
SLC25A5	1.05	Ns	1.34	Ns	Adenine nucleotide translocation
SOD1	**0.20**	0.001	**0.38**	0.02	ROS protection (cytosol)
SOD2	**0.42**	0.001	**0.40**	0.05	ROS protection (mitochondria)
STARD3	0.86	0.02	**0.45**	0.02	Cholesterol import
TIMM10	1.56	0.01	1.20	Ns	Protein insertion in the inner membrane
TIMM17A	1.71	0.001	0.95	Ns	Protein insertion in the inner membrane

TIMM17B	1.63	0.02	0.79	0.01	Protein insertion in the inner membrane
TIMM8A	1.67	0.02	1.00	Ns	Protein insertion in the inner membrane
TIMM8B	**3.63**	0.001	1.74	0.05	Protein insertion in the inner membrane
TIMM9	0.60	Ns	1.20	Ns	Protein insertion in the inner membrane
TOMM20	**0.41**	0.01	**0.20**	0.001	Mitochondrial proteins import
TOMM22	1.67	0.01	1.20	Ns	Mitochondrial proteins import
TOMM34	1.21	Ns	1.51	Ns	Mitochondrial proteins import
TOMM40	1.67	0.02	**0.40**	0.02	Mitochondrial proteins import
TOMM70A	1.21	Ns	1.09	Ns	Mitochondrial proteins import
TSPO	1.13	Ns	1.15	Ns	Cholesterol import
UCP1	**3.46**	0.001	**3.17**	0.002	OXPHOS/ATP synthesis uncoupling
UCP2	**4.12**	0.001	**3.44**	0.001	OXPHOS/ATP synthesis uncoupling
UCP3	**4.12**	0.001	**3.18**	0.005	OXPHOS/ATP synthesis uncoupling
UQCR11	1.39	0.005	1.60	0.001	Ubiquinol-cytochrome c reductase subunit
UQCRC1	1.49	0.002	1.30	0.01	Ubiquinol-cytochrome c reductase subunit
UQCRC2	1.06	Ns	1.60	0.001	Ubiquinol-cytochrome c reductase subunit
UQRCFS1	**0.42**	0.001	0.68	0.001	Ubiquinol-cytochrome c reductase subunit
UQCRH	1.60	0.001	1.11	0.05	Ubiquinol-cytochrome c reductase subunit
UQCRQ	1.13	Ns	0.92	Ns	Ubiquinol-cytochrome c reductase subunit

Ctrl: untreated cells; Dox: cells treated with 5 μmol/L Dox for 24 h; mtDox: cells treated with 5 μmol/L mtDox for 24 h; OXPHOS: oxidative phosphorylation.
Fold-Change (2^(- Delta Delta Ct)) is the normalized gene expression (2^(- Delta Ct)) in Dox- or mtDox-treated U-2OS cells, divided the normalized gene expression (2^(- Delta Ct)) in untreated cells (n= 4), where Ct is the threshold cycle in qRT-PCR; when the fold-change is less than 1, the value was the negative inverse of the fold-change. Ns: not significant. Bold characters: up- or down-regulation more than two-fold.

Supplementary Table S4. Expression of mitochondria-related genes in U-2OS/DX580 cells untreated and treated with doxorubicin or mitochondria-targeted doxorubicin

Gene	Fold change Dox versus Ctrl	p value	Fold change mtDox versus Ctrl	p value	Biological function
AIFM2	1.58	Ns	0.71	0.002	Apoptosis induction
ATP12A	1.22	Ns	**0.23**	0.001	H^+/ATP exchange
ATP4A	1.26	Ns	**0.21**	0.001	H^+/ATP exchange
ATP4B	1.28	Ns	**0.21**	0.001	H^+/ATP exchange
ATP50	1.66	0.05	1.62	0.001	ATP synthase subunit
ATP5A1	1.67	0.01	1.46	0.001	ATP synthase subunit
ATP5B	1.34	0.02	1.31	0.01	ATP synthase subunit
ATP5C1	1.22	Ns	1.44	0.001	ATP synthase subunit
ATP5F1	**2.01**	0.02	1.76	0.002	ATP synthase subunit
ATP5G1	1.26	Ns	0.76	0.005	ATP synthase subunit
ATP5G2	1.37	Ns	**0.41**	0.001	ATP synthase subunit
ATP5G3	0.89	Ns	0.51	0.001	ATP synthase subunit
ATP5I	1.11	Ns	1.23	Ns	ATP synthase subunit
ATP5J	1.26	0.05	1.62	0.005	ATP synthase subunit
ATP5J2	**2.07**	0.01	**0.22**	0.001	ATP synthase subunit
ATP5L	1.21	0.02	**0.33**	0.001	ATP synthase subunit
BAK1	1.00	Ns	**2.72**	0.001	Apoptosis induction
BBC3	1.23	Ns	**2.19**	0.001	Apoptosis induction
BCL2	1.03	0.05	**0.43**	0.001	Apoptosis inhibition
BCL2L1	0.93	Ns	**0.29**	0.005	Apoptosis inhibition
BCS1L	0.66	0.05	**0.41**	0.001	Ubiquinol-cytochrome c reductase assembly
BID	1.89	0.05	**2.76**	0.01	Apoptosis induction
BNIP3	1.26	Ns	**2.09**	0.05	Apoptosis induction
COX10	1.44	Ns	1	Ns	Cytochrome c oxidase assembly
COX18	0.72	0.02	0.66	0.05	Cytochrome c oxidase assembly
COX412	1.21	Ns	**0.20**	0.001	Cytochrome c oxidase subunit
COX4I1	**2.11**	0.01	**2.14**	0.001	Cytochrome c oxidase assembly
COX5A	1.78	0005	1.86	0.001	Cytochrome c oxidase subunit
COX5B	1.09	Ns	1.11	Ns	Cytochrome c oxidase subunit
COX6A1	0.98	Ns	**0.41**	0.001	Cytochrome c oxidase subunit
COX6A2	1.00	Ns	**0.29**	0.001	Cytochrome c oxidase subunit
COX6B1	0.92	Ns	1.20	0.05	Cytochrome c oxidase assembly/regulation
COX6C	1.21	Ns	**0.43**	0.001	Cytochrome c oxidase assembly/regulation
COX7A2	1.23	Ns	1.23	Ns	Cytochrome c oxidase assembly/regulation
COX7A2L	1.26	Ns	1.28	0.02	Cytochrome c oxidase assembly/regulation
COX7B	1.39	Ns	1.41	0.02	Cytochrome c oxidase subunit

COX8A	1.30	Ns	1.51	0.02	Cytochrome c oxidase regulation
CPT1	1.04	0.05	**0.24**	0.05	Long chain fatty acylcoA import/β-oxidation
CPT2	0.81	Ns	**0.37**	0.02	Long chain fatty acylcoA import/β-oxidation
CYC1	1.51	0.002	1.23	Ns	Electron transport
DMM1L	1.04	Ns	1.24	Ns	Control of mitochondria morphology
FIS1	1.44	Ns	1.06	Ns	Control of mitochondria fission
FXC1	1.55	0.02	**0.40**	0.05	Mitochondrial proteins import
HSP90A1	1.44	Ns	1.20	Ns	Proteins chaperon
HSPD1	1.15	Ns	1.09	Ns	Mitochondrial proteins chaperon
IMMP1L	1.79	0.01	**0.41**	0.005	Mitochondrial proteins processing/import
IMMP2L	1.81	Ns	1.82	Ns	Mitochondrial proteins processing/import
LRPPRC	0.91	Ns	0.95	Ns	Mitochondrial transcription factor
MFN1	0.95	Ns	**0.36**	0.05	Control of mitochondria fusion
MFN2	0.83	0.05	**0.39**	0.02	Control of mitochondria fusion
MIPEP	1.05	Ns	0.79	Ns	Mitochondrial proteins processing
MPV17	0.79	0.01	1.15	Ns	Metabolism of mitochondrial ROS
MTX2	**0.45**	0.02	**0.31**	0.02	Mitochondrial proteins import
NDUFA1	0.77	0.01	1.23	0.005	NADH:ubiquinone oxidoreductase subunit
NDUFA10	0.97	Ns	0.76	0.005	NADH:ubiquinone oxidoreductase subunit
NDUFA11	1.56	0.005	1.62	0.001	NADH:ubiquinone oxidoreductase subunit
NDUFA2	1.34	0.01	**0.29**	0.001	NADH:ubiquinone oxidoreductase assembly
NDUFA3	1.51	0.01	**0.08**	0.001	NADH:ubiquinone oxidoreductase subunit
NDUFA4	1.13	Ns	1.29	Ns	NADH:ubiquinone oxidoreductase subunit
NDUFA5	1.78	0.02	1.63	0.001	NADH:ubiquinone oxidoreductase subunit
NDUFA6	1.30	0.05	1.51	0.001	NADH:ubiquinone oxidoreductase subunit
NDUFA7	1.24	Ns	1.17	0.05	NADH:ubiquinone oxidoreductase subunit
NDUFA8	1.61	0.001	1.02	Ns	NADH:ubiquinone oxidoreductase subunit
NDUFAB1	1.23	Ns	1.41	0.001	NADH:ubiquinone oxidoreductase subunit
NDUFAB10	1.45	0.05	1.15	Ns	NADH:ubiquinone oxidoreductase subunit
NDUFB2	1.42	0.05	1.71	0.05	NADH:ubiquinone oxidoreductase subunit
NDUFB3	1.26	0.05	**0.50**	0.02	NADH:ubiquinone oxidoreductase subunit
NDUFB4	1.84	0.02	0.63	0.05	NADH:ubiquinone oxidoreductase subunit
NDUFB5	1.23	Ns	**0.40**	0.01	NADH:ubiquinone oxidoreductase subunit
NDUFB6	1.56	Ns	1.14	Ns	NADH:ubiquinone oxidoreductase subunit
NDUFB7	1.56	0.05	1.41	0.01	NADH:ubiquinone oxidoreductase subunit
NDUFB8	1.29	0.05	1.99	0.005	NADH:ubiquinone oxidoreductase subunit
NDUFB9	0.78	0.05	0.81	0.02	NADH:ubiquinone oxidoreductase subunit
NDUFC1	1.42	0.01	1.41	0.001	NADH:ubiquinone oxidoreductase subunit
NDUFC2	1.60	0.01	1.23	0.005	NADH:ubiquinone oxidoreductase subunit
NDUFS1	1.72	0.002	1.46	0.001	NADH:ubiquinone oxidoreductase subunit
NDUFS2	1.11	Ns	1.74	0.001	NADH:ubiquinone oxidoreductase subunit
NDUFS3	0.78	Ns	**0.24**	0.001	NADH:ubiquinone oxidoreductase subunit

NDUFS4	1.62	0.001	1.13	Ns	NADH:ubiquinone oxidoreductase subunit
NDUFS5	1.28	0.05	**0.38**	0.005	NADH:ubiquinone oxidoreductase subunit
NDUFS6	1.36	Ns	1.46	0.001	NADH:ubiquinone oxidoreductase subunit
NDUFS7	1.17	Ns	1.51	0.002	NADH:ubiquinone oxidoreductase subunit
NDUFS8	**2.11**	0.05	**3.46**	0.001	NADH:ubiquinone oxidoreductase subunit
NDUFV1	1.01	Ns	**0.37**	0.001	NADH:ubiquinone oxidoreductase subunit
NDUFV2	1.32	Ns	1.12	Ns	NADH:ubiquinone oxidoreductase subunit
NDUFV3	0.71	Ns	0.81	Ns	NADH:ubiquinone oxidoreductase subunit
OPA1	1.02	0.002	**0.16**	0.001	Control of mitochondria network
OXA1L	1.56	0.02	**0.46**	0.005	Cytochrome c oxidase assembly
RHOT1	0.63	0.01	0.52	0.05	Control of mitochondria fission and fusion
RHOT2	1.16	0.001	**0.22**	0.05	Control of mitochondria fission and fusion
SDHA	1.32	Ns	0.61	0.001	Succinate dehydrogenase subunit
SDHB	1.89	0.001	1.34	0.001	Succinate dehydrogenase subunit
SDHC	1.42	0.002	0.87	0.05	Succinate dehydrogenase subunit
SDHD	1.70	0.002	1.99	0.001	Succinate dehydrogenase subunit
SH3SGLB1	1.32	Ns	1.51	0.05	Apoptosis induction
SLC25A1	0.79	0.005	0.56	0.01	Tricarboxylic acids import
SLC25A10	1	Ns	**0.46**	0.005	Mitochondrial proteins import
SLC25A12	0.83	0.05	**0.49**	0.005	Dicarboxylic acids import
SLC25A13	0.76	0.01	**0.42**	0.01	Aspartic acid/glutamic acid exchange
SLC25A14	1.91	0.005	0.56	0.005	Aspartic acid/glutamic acid exchange
SLC25A15	1.71	Ns	**0.29**	0.001	Ornithine import
SLC25A19	1.32	Ns	1.09	Ns	Thiamine pyrophosphate import
SLC25A2	**0.10**	0.05	**0.19**	0.05	Mitochondrial proteins import
SLC25A20	1.07	Ns	**0.45**	0.05	Carnitine/acylcarnitine translocation
SLC25A21	0.72	0.01	0.76	0.05	Oxodicarboxylic acids import
SLC25A22	1.69	0.01	**0.40**	0.05	Glutamate import
SLC25A23	1.32	Ns	1.26	Ns	Phosphate import
SLC25A24	1.15	Ns	0.70	Ns	Phosphate import
SLC25A25	1.45	0.002	**0.41**	0.05	Phosphate import
SLC25A27	1.18	Ns	**2.45**	0.02	OXPHOS/ATP synthesis uncoupling
SLC25A3	1.38	Ns	1.51	Ns	Phosphate/hydroxyl ions exchange
SLC25A31	0.72	0.005	1.09	Ns	Adenine nucleotide translocation
SLC25A37	0.81	0.05	**0.21**	0.002	Iron import
SLC25A4	1.74	0.05	1.32	Ns	Adenine nucleotide translocation
SLC25A5	1.26	Ns	1.58	Ns	Adenine nucleotide translocation
SOD1	1.38	Ns	0.38	Ns	ROS protection (cytosol)
SOD2	1.09	Ns	**0.40**	0.05	ROS protection (mitochondria)
STARD3	1.00	0.02	**0.45**	0.02	Cholesterol import
TIMM10	1.26	Ns	1.20	Ns	Protein insertion in the inner membrane
TIMM17A	1.04	Ns	0.75	Ns	Protein insertion in the inner membrane

TIMM17B	1.26	Ns	**0.49**	0.01	Protein insertion in the inner membrane
TIMM8A	1.15	Ns	**0.41**	0.005	Protein insertion in the inner membrane
TIMM8B	1.58	Ns	1.74	0.05	Protein insertion in the inner membrane
TIMM9	1.32	Ns	1.20	Ns	Protein insertion in the inner membrane
TOMM20	0.87	Ns	1.20	Ns	Mitochondrial proteins import
TOMM22	**0.40**	0.02	**0.21**	0.001	Mitochondrial proteins import
TOMM34	1.51	Ns	1.51	Ns	Mitochondrial proteins import
TOMM40	1.06	0.005	**0.33**	0.05	Mitochondrial proteins import
TOMM70A	1.20	Ns	**0.47**	0.02	Mitochondrial proteins import
TSPO	1.09	Ns	**0.17**	0.005	Cholesterol import
UCP1	1.21	Ns	**2.19**	0.05	OXPHOS/ATP synthesis uncoupling
UCP2	1.66	0.05	1.44	Ns	OXPHOS/ATP synthesis uncoupling
UCP3	1.21	Ns	**2.18**	0.05	OXPHOS/ATP synthesis uncoupling
UQCR11	1.34	Ns	0.93	Ns	Ubiquinol-cytochrome c reductase subunit
UQCRC1	1.65	0.005	1.62	0.001	Ubiquinol-cytochrome c reductase subunit
UQCRC2	1.32	0.05	**0.32**	0.001	Ubiquinol-cytochrome c reductase subunit
UQRCFS1	1.72	0.05	**0.30**	0.001	Ubiquinol-cytochrome c reductase subunit
UQCRH	1.19	Ns	1.15	Ns	Ubiquinol-cytochrome c reductase subunit
UQCRQ	0.89	Ns	**0.46**	0.01	Ubiquinol-cytochrome c reductase subunit

Ctrl: untreated cells; Dox: cells treated with 5 μmol/L Dox for 24 h; mtDox: cells treated with 5 μmol/L mtDox for 24 h; OXPHOS: oxidative phosphorylation.
Fold-Change (2^(- Delta Delta Ct)) is the normalized gene expression (2^(- Delta Ct)) in Dox- or mtDox-treated U-2OS/DX580 cells, divided the normalized gene expression (2^(- Delta Ct)) in untreated cells (n= 4), where Ct is the threshold cycle in qRT-PCR; when the fold-change is less than 1, the value is the negative inverse of the fold-change. Ns: not significant. Bold characters: up- or down-regulation more than two-fold.

Supplementary Tables S5. qRT-PCR validation of PCR-arrays results in U-2OS, U-2OS/DX30, U-2OS/DX100, U-2OS/DX580 cells

Gene name	Relative expression U-2OS/DX30 vs U-2OS	Relative expression U-2OS/DX30 vs U-2OS	Relative expression U-2OS/DX30 vs U-2OS	Biological function
TIMM8B	1.92 ± 0.32 *	2.89 ± 0.34 *	5.01 ± 0.47 *	Protein insertion in the inner membrane
TOMM70A	1.72 ± 0.21 *	1.81 ± 0.29 *	3.34 ± 0.27 *	Mitochondrial proteins import
MFN2	2.92 ± 0.37 *	2.82 ± 0.71 *	3.72 ± 0.52 *	Control of mitochondria fusion
OPA1	1.26 ± 0.12	1.54 ± 0.12 *	2.91 ± 0.43 *	Control of mitochondria network
SLC25A10	2.12 ± 0.61 *	2.73 ± 0.37 *	5.88 ± 0.34 *	Dicarboxylic acids import
CPT1	1.52 ± 0.26	2.44 ± 0.23 *	3.17 ± 0.28 *	Long chain fatty acylcoA import/β-oxidation
NDUFA2	1.43 ± 0.21	5.03 ± 0.47 *	5.99 ± 0.71 *	NADH:ubiquinone oxidoreductase assembly
NDUFS5	2.35 ± 0.36 *	2.67 ± 0.11 *	5.56 ± 0.43 *	NADH:ubiquinone oxidoreductase subunit
UQRCQ	1.76 ± 0.33 *	1.82 ± 0.32 *	2.47 ± 0.55 *	Ubiquinol-cytochrome c reductase subunit
UQRCFS1	2.21 ± 0.65 *	7.13 ± 1.29 *	13.09 ± 2.24 *	Ubiquinol-cytochrome c reductase subunit
OXA1L	1.26 ± 0.21	2.53 ± 0.12 *	4.82 ± 0.33 *	Cytochrome c oxidase assembly
ATP5L	3.67 ± 0.56 *	4.45 ± 0.87 *	8.33 ± 1.21 *	ATP synthase subunit
UCP1	2.02 ± 0.35 *	1.18 ± 0.21	0.19 ± 0.05 *	OXPHOS/ATP synthesis uncoupling
SLC25A27	0.62 ± 0.12 *	0.26 ± 0.11 *	0.13 ± 0.06 *	OXPHOS/ATP synthesis uncoupling
SOD2	1.54 ± 0.31	2.28 ± 0.54 *	3.66 ± 0.29 *	ROS protection (mitochondria)
BAK1	1.23 ± 0.22	1.09 ± 0.03	0.98 ± 0.15	Apoptosis induction
BCL2	0.93 ± 0.21	1.22 ± 0.11	1.32 ± 0.09	Apoptosis inhibition

The expression levels of specific mitochondria-related genes, representative of the main biological categories screened by PCR arrays (Supplementary Table S2), were validated by qRT-PCR (n = 3). The expression level of each gene in U-2OS cells was considered as 1. The relative expression of the other genes was calculated with PrimePCR™ Analysis Software. *S14* gene was used as the housekeeping gene. Versus U-2OS cells: * $p < 0.05$.

Supplementary Tables S6. qRT-PCR validation of PCR-arrays results in U-2OS cells treated with doxorubicin or mitochondria-targeted doxorubicin

Gene name	Relative expression Dox vs Ctrl	Relative expression mtDox vs Ctrl	Biological function
TIMM8B	3.56 ± 0.34 *	1.65 ± 0.41	Protein insertion in the inner membrane
TOMM70A	1.12 ± 0.11	1.34 ± 0.26	Mitochondrial proteins import
MFN2	1.11 ± 0.19	0.27 ± 0.11 *	Control of mitochondria fusion
OPA1	0.79 ± 0.27	0.51 ± 0.09 *	Control of mitochondria network
SLC25A10	3.09 ± 0.45 *	0.62 ± 0.20 *	Dicarboxylic acids import
CPT1	0.32 ± 0.11 *	0.19 ± 0.08 *	Long chain fatty acylcoA import/β-oxidation
NDUFA2	1.83 ± 0.14 *	1.89 ± 0.25 *	NADH:ubiquinone oxidoreductase assembly
NDUFS5	1.27 ± 0.06	1.35 ± 0.09	NADH:ubiquinone oxidoreductase subunit
UQRCQ	1.01 ± 0.28	1.14 ± 0.28	Ubiquinol-cytochrome c reductase subunit
UQRCFS1	0.59 ± 0.18 *	0.63 ± 0.12 *	Ubiquinol-cytochrome c reductase subunit
OXA1L	0.92 ± 0.31	0.42 ± 0.11 *	Cytochrome c oxidase assembly
ATP5L	1.57 ± 0.33	1.26 ± 0.05	ATP synthase subunit
UCP1	3.01 ± 0.72 *	3.35 ± 0.61 *	OXPHOS/ATP synthesis uncoupling
SLC25A27	2.13 ± 0.27 *	2.61 ± 0.64 *	OXPHOS/ATP synthesis uncoupling
SOD2	0.61 ± 0.18 *	0.42 ± 0.19 *	ROS protection (mitochondria)
BAK1	2.93 ± 0.34 *	3.37 ± 0.71 *	Apoptosis induction
BCL2	0.39 ± 0.12 *	0.18 ± 0.08 *	Apoptosis inhibition

The expression levels of specific mitochondria-related genes, representative of the main biological categories screened by PCR arrays (Supplementary Table S3), were validated by qRT-PCR (n = 3). The expression level of each gene in untreated U-2OS cells was considered as 1. The relative expression of the other genes was calculated with PrimePCR™ Analysis Software. *S14* gene was used as the housekeeping gene. Versus untreated U-2OS cells: * $p < 0.05$.

Supplementary Tables S7. qRT-PCR validation of PCR-arrays results in U-2OS/DX580 cells treated with doxorubicin or mitochondria-targeted doxorubicin

Gene name	Relative expression Dox vs Ctrl	Relative expression mtDox vs Ctrl	Biological function
TIMM8B	1.28 ± 0.21	1.54 ± 0.33	Protein insertion in the inner membrane
TOMM70A	1.07 ± 0.21	0.52 ± 0.13 *	Mitochondrial proteins import
MFN2	0.95 ± 0.13	0.43 ± 0.18 *	Control of mitochondria fusion
OPA1	0.91 ± 0.08	0.21 ± 0.10 *	Control of mitochondria network
SLC25A10	1.14 ± 0.21	0.33 ± 0.06 *	Dicarboxylic acids import
CPT1	0.95 ± 0.18	0.26 ± 0.05 *	Long chain fatty acylcoA import/β-oxidation
NDUFA2	1.04 ± 0.12	0.21 ± 0.03 *	NADH:ubiquinone oxidoreductase assembly
NDUFS5	1.04 ± 0.19	0.41 ± 0.23 *	NADH:ubiquinone oxidoreductase subunit
UQRCQ	1.08 ± 0.11	0.61 ± 0.15 *	Ubiquinol-cytochrome c reductase subunit
UQRCFS1	1.52 ± 0.13	0.33 ± 0.07 *	Ubiquinol-cytochrome c reductase subunit
OXA1L	1.24 ± 0.11	0.61 ± 0.17 *	Cytochrome c oxidase assembly
ATP5L	1.06 ± 0.14	0.41 ± 0.19 *	ATP synthase subunit
UCP1	1.17 ± 0.25	2.49 ± 0.36 *	OXPHOS/ATP synthesis uncoupling
SLC25A27	0.97 ± 0.21	2.27 ± 0.31 *	OXPHOS/ATP synthesis uncoupling
SOD2	0.87 ± 0.11	0.36 ± 0.14 *	ROS protection (mitochondria)
BAK1	1.32 ± 0.22	3.11 ± 0.39 *	Apoptosis induction
BCL2	1.059 ± 0.19	0.37 ± 0.13 *	Apoptosis inhibition

The expression levels of specific mitochondria-related genes, representative of the main biological categories screened by PCR arrays (Supplementary Table S4), were validated in qRT-PCR (n = 3). The expression level of each gene in untreated U-2OS/DX580 cells was considered as 1. The relative expression of the other genes was calculated with PrimePCR™ Analysis Software. *S14* gene was used as the housekeeping gene. Versus untreated U-2OS/DX580 cells: * $p < 0.05$.